

Validated matrix multiplication transform for orthogonal polynomials with applications to computer-assisted proofs for PDEs

Matthieu Cadiot*

Jonathan Jaquette†

Jean-Philippe Lessard‡

Akitoshi Takayasu§

November 28, 2024

Abstract

In this paper, we achieve three primary objectives related to the rigorous computational analysis of nonlinear PDEs posed on complex geometries such as disks and cylinders. First, we introduce a validated Matrix Multiplication Transform (MMT) algorithm, analogous to the discrete Fourier transform, which offers a reliable framework for evaluating nonlinearities in spectral methods while effectively mitigating challenges associated with rounding errors. Second, we examine the Zernike polynomials, a spectral basis well-suited for problems on the disk, and highlight their essential properties. We further demonstrate how the MMT approach can be effectively employed to compute the product of truncated Zernike series, ensuring both accuracy and efficiency. Finally, we combine the MMT framework and Zernike series to construct computer-assisted proofs that establish the existence of solutions to two distinct nonlinear elliptic PDEs on the disk.

Keywords. Matrix Multiplication Transform, Orthogonal Polynomials, Gaussian Quadrature, Zernike Series, Computer-Assisted Proofs, Elliptic PDEs on the Disk

1 Introduction

The study of partial differential equations (PDEs) has long been a central topic in mathematics and applied sciences. Many of these equations, especially nonlinear ones, do not admit closed-form solutions, making their analysis and numerical resolution essential for practical applications. In recent years, computer-assisted proofs (CAPs) have emerged as a powerful tool to rigorously establish the existence of solutions to PDEs. The objective of CAPs is to combine numerical methods with rigorous mathematical analysis to provide precise, verified solutions, thereby bridging the gap between computational results and analytical proofs. By analyzing the solutions in an appropriately chosen space, CAPs offer a means to rigorously verify the existence of solutions expressed as expansions within a given basis. The challenge lies not only in obtaining a good

*Department of Mathematics and Statistics, McGill University, Montreal, QC, H3A 0B9, Canada (matthieu.cadiot@mail.mcgill.ca)

†New Jersey Institute of Technology, University Heights, Cullimore Hall 606, Newark, New Jersey, 07102, USA (jonathan.jaquette@njit.edu)

‡Department of Mathematics and Statistics, McGill University, Montreal, QC, H3A 0B9, Canada (jp.lessard@mcgill.ca)

§Institute of Systems and Information Engineering, University of Tsukuba, 1-1-1 Tennodai, Tsukuba, Ibaraki 305-8573, Japan (takitoshi@risk.tsukuba.ac.jp)

numerical approximation but also in ensuring that the solution is valid in a rigorous sense, respecting the underlying geometry of the problem and the specific properties of the PDE.

The field of CAPs in PDEs may be seen as part of a larger global effort to construct rigorous proofs for nonlinear dynamical systems. Early pioneering works, such as those on the Feigenbaum conjectures [Lan82] and the existence of chaos and global attractors in the Lorenz equations [MM95b, Tuc21, Tuc99], as well as more recent proofs of Jones’ and Wright’s conjectures in delay equations [Jaq19, vdBJ18], chaos in the 1D Kuramoto-Sivashinsky PDE [WZ20], and instability proofs in Poiseuille flow [WPN09], have laid the groundwork for this field. Additionally, the study of bifurcating solutions for 3D Rayleigh-Bénard problems [KNWN09], equilibria in the 3D Navier-Stokes (NS) equations [LNO22], solutions of NS on unbounded strips with obstacles [Wun22], 3D gyroid patterns in materials [vdBW19], periodic orbits in NS [vdBBLvV21], blowup in Euler equations on the cylinder [CH22], and imploding solutions for 3D compressible fluids [BCLGS22], further underscore the growing importance of CAPs in analyzing nonlinear systems. For more details, we refer the interested reader to the book [NPW19] and the survey papers [KSW96, vdBL15, GS19]. It is worth mentioning that a fundamental tool in these CAPs is the use of interval arithmetic [Moo66], which efficiently ensures that all floating-point errors are controlled in the computations, thus guaranteeing the reliability of the results.

A crucial aspect of solving PDEs is the choice of basis functions in which the solution is expanded. The choice of basis function depends heavily on the geometry of the domain, the boundary conditions imposed, and the differential operators involved. For simple geometries, such as periodic domains or intervals, standard bases such as Fourier series or Chebyshev polynomials are often sufficient. For instance, on a periodic domain, Fourier basis functions are optimal, due to their simple form under differentiation and their good approximation properties. Similarly, on a one-dimensional compact interval, Chebyshev polynomials (essentially Fourier cosine series, as discussed in [Boy01]) are widely used, particularly when boundary conditions are not periodic. However, when dealing with more complex domains — such as disks, spheres, or other non-Euclidean geometries — the selection of an appropriate basis becomes less straightforward. The Fourier basis, though highly effective for periodic problems, is not universally applicable in these cases. In such settings, the geometry of the problem suggests the use of specialized basis functions, which may include non-polynomial options like Bessel functions or Hermite functions, or polynomial options such as Legendre polynomials or generalized Jacobi polynomials. Each of these bases has its own advantages and drawbacks, making the choice of basis a key consideration in the numerical resolution of the PDE.

In the field of CAPs for PDEs, two distinct approaches have traditionally been employed (we refer the interested reader to the recent survey paper [GS19] for a comprehensive discussion of the topic). First, finite element methods have been widely used to analyze PDEs defined on complex geometries [YN93, NHW05, LO13, TLO13, NPW19, Wun22]. This approach is highly versatile, as it allows for the consideration of more general domains. However, it comes with the tradeoff of lacking strong approximation properties, which often limits the scope of CAP results to relatively simple dynamical objects, such as steady states and their stability. Second, there exists a long tradition of studying PDEs on toroidal or rectangular domains using Fourier series [ZM01, GL10, AK10, vdBW19, AGK21]. The main advantage of this approach lies in the excellent approximation properties of spectral methods, including spectral convergence. This enables the analysis of more complex dynamical systems, such as periodic orbits [FGLdLL17, vdBBLvV21], connecting orbits [CW18] and chaos [WZ20]. However, the major limitation is that the Fourier approach is typically limited to restricted geometries, where the domain is rectangular or periodic.

Classical topics in PDEs explore complex dynamical behaviors across a broad range of geometries, such as spiral waves in excitable media [SSW99] and the axisymmetric Navier-Stokes

equations [Lop94, Hou23]. However, a gap remains in the literature on CAPs with respect to the development of spectral methods for such geometries. One key challenge in cylindrical and spherical domains is the apparent singularity introduced by polar coordinates. Previous work in the CAPs literature has addressed this difficulty by utilizing Taylor series expansions [vdBDL22, vdBBC⁺18]. Recent efforts have sought to bridge this gap by establishing a framework for developing CAPs based on global spectral bases [AK19, BC24, AK24]. In [AK19], which focused on solutions on a disk, the authors noted that expanding the radial variable as a Chebyshev series proved effective as a pseudospectral method, but it was only by employing Zernike series that they successfully produced a CAP. In their subsequent work [AK24], they used spherical harmonics as a basis to construct CAPs for periodic and quasi-periodic solutions on the sphere. Their results demonstrate that by combining spectral methods with rigorous error bounds, it is possible to establish the existence of solutions to elliptic and parabolic PDEs in geometries that were previously not considered in earlier studies.

Given the inherently nonlinear nature of many PDEs encountered in real-world applications, it is crucial to handle the nonlinear terms with care within the framework of CAPs. To address this challenge, the present work establishes a framework for rigorously evaluating nonlinearities within a chosen basis through the introduction of a validated *Matrix Multiplication Transform* (MMT) approach [Boy01]. Similar to the discrete Fourier transform (DFT), the MMT approach facilitates the transformation of a function’s representation between its coefficients in a given basis (where derivative evaluations are straightforward) and its values at carefully selected grid points (where nonlinearities are more easily evaluated). The MMT provides a precise and computationally efficient method for evaluating nonlinear terms, which is typically a computationally intensive task requiring sophisticated error analysis. In the context of PDEs posed on higher-dimensional domains, where solutions are represented using a tensor product of bases, the coefficients-to-grid transformation can be performed through a sequence of one-dimensional transforms, leading to significant computational savings. Therefore, in this paper, we focus on developing the MMT approach specifically in the context of one-dimensional polynomials.

To describe the MMT approach in detail, fix a one-dimensional polynomial basis $\{p_n\}_{n=0}^{\infty}$ on the interval $[a, b]$ such that the degree of p_n is n , and consider a polynomial $f : [a, b] \rightarrow \mathbb{R}$

$$f(x) = \sum_{n=0}^N a_n p_n(x), \quad (1)$$

given as a linear combination of basis polynomial functions $p_n(x)$. We aim to rigorously evaluate a nonlinear transformation $\mathcal{G}(f(x))$, where \mathcal{G} is a polynomial nonlinear function, such as $\mathcal{G}(f(x)) = f(x)^2$. That is, we wish to derive an exact formula for the expansion:

$$\mathcal{G}(f(x)) = \sum_{n=0}^{N'} c_n p_n(x), \quad (2)$$

where N' is sufficiently large (e.g. if f is degree N and \mathcal{G} is degree d , then $N' = dN$).

The MMT approach provides a structured and efficient way to handle such nonlinear evaluations rigorously. Summarized in Figure 1, our approach involves: (i) evaluating f on a carefully selected grid; (ii) applying the nonlinearity to obtain the values of $\mathcal{G}(f)$ on the grid; and (iii) applying an inverse transform to yield the coefficients of $\mathcal{G}(f)$ expanded in the basis $\{p_n\}_{n=0}^{N'}$. We denote the *Matrix Multiplication Transform* (MMT) as the mapping from coefficient-space to grid-space, and the *inverse Matrix Multiplication Transform* (iMMT) as the mapping from grid-space to coefficient-space.

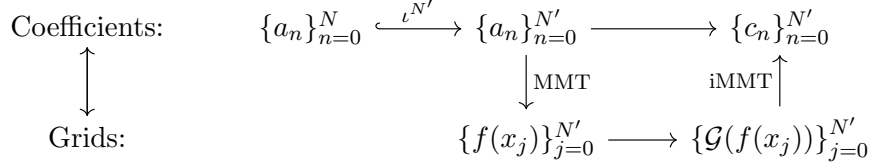


Figure 1: Diagram of evaluating the polynomial nonlinearity \mathcal{G} via the MMT approach.

Definition 1.1 (Matrix Multiplication Transform). Let $\mathbf{a} = (a_0, \dots, a_N)^T$ be the vector of coefficients of the finite sum of polynomials in (1), and let $\mathbf{f} \stackrel{\text{def}}{=} (f(x_0), \dots, f(x_N))^T$ be the vector of grid values of (1) at distinct nodes $\{x_j\}_{j=0}^N$.

- Define $M : \mathbf{a} \mapsto \mathbf{f}$, which maps the coefficients \mathbf{a} to the grid values \mathbf{f} , to be the MMT matrix.
- Define $M^{-1} : \mathbf{f} \mapsto \mathbf{a}$, which maps the grid values to coefficients, to be the iMMT matrix.

As the polynomials $\{p_j\}_{j=0}^N$ are linearly independent and nodes $\{x_j\}_{j=0}^N$ are distinct, it follows that M is an invertible, linear map, and may be represented as an $(N+1) \times (N+1)$ matrix. Moreover, each entry of the MMT matrix M is universally defined as

$$(M)_{j,n} \stackrel{\text{def}}{=} p_n(x_j), \quad (3)$$

for $0 \leq j, n \leq N$, where j represents the row index and n represents the column index of M . In this manner, we are able to obtain the grid values via the matrix-vector product $\mathbf{f} = M\mathbf{a}$.

An essential consideration for CAPs is the effect of aliasing. The MMT is only an invertible transformation between the space of polynomials of degree at most N , and their values on nodes $\{x_j\}_{j=0}^N$. However if f is degree N and \mathcal{G} is degree d , then $\mathcal{G}(f)$ will be a degree $N' = dN$ polynomial. To dealias our results, we need to evaluate the nonlinearity \mathcal{G} at the polynomial f on a set of grid points $\{x_j\}_{j=0}^{N'}$. Hence, a preliminary step in the MMT approach is to pad the coefficients $\{a_n\}_{n=0}^N$ with zeros, mapping it to $\{a_n\}_{n=0}^{N'} \stackrel{\text{def}}{=} \iota^{N'}(\{a_n\}_{n=0}^N)$, where the inclusion $\iota^{N'} : \mathbb{R}^{N+1} \rightarrow \mathbb{R}^{N'+1} \times \mathbb{R}^{N'-N}$ is the zero section. Subsequently, the $(N'+1) \times (N'+1)$ MMT matrix enables us to transform the coefficients $\{a_n\}_{n=0}^{N'}$ to grid values $\{f(x_j)\}_{j=0}^{N'}$. The nonlinearity is then evaluated at the grid points (i.e., $f(x_j) \mapsto \mathcal{G}(f(x_j))$), and finally, the values $\mathcal{G}(f(x_j))$ are transformed back via the iMMT to obtain the coefficients c_n (see Figure 1).

The selection of grid points $\{x_j\}_{j=0}^{N'}$ and polynomials $\{p_n(x)\}_{n=0}^{N'}$ is crucial for ensuring well-conditioned MMT matrices. For instance, if we choose monomials $p_n(x) = x^n$ and an equally spaced grid, the resulting matrix M becomes a Vandermonde matrix, which is typically ill-conditioned, especially for large N . Therefore, making careful choices for these elements is essential. Classical Gaussian quadrature theory suggests that better conditioning can be achieved by selecting orthogonal polynomials $\{p_n(x)\}$ and placing the nodes $\{x_j\}_{j=0}^{N'}$ at the zeros of the corresponding polynomial of degree $N'+1$. However, even in this case, implementing the algorithms with validated numerics remains ill-conditioned and presents significant challenges for obtaining practical results [Sto93].

In Section 2, we propose a general strategy for overcoming these difficulties. We provide explicit formulas for the entries of the iMMT matrix and introduce computable methods for efficiently calculating these entries. In particular, we provide in Section 3 a computer-assisted approach based on validated numerics to make such computations rigorous. We present a quantitative comparison of the different computable methods for computing the MMT and their relative propagation of error when using interval arithmetic. Such an analysis is essential in view of treating nonlinear PDE problems.

Remark 1.2 (Clebsch-Gordon vs MMT). *We note that when the polynomials p_n in (1) are orthogonal, a conventional approach for evaluating $\mathcal{G}(f(x))$ employs Clebsch-Gordon (or linearization) coefficients [BLC84, AK19]. These coefficients are defined through the relation $p_i(x)p_j(x) = \sum_{|i-j| \leq k \leq |i+j|} c_{i,j}^k p_k(x)$. However, this method generically incurs a computational complexity of $\mathcal{O}(N^3)$ for each product evaluation. In contrast, our MMT approach reduces this complexity to $\mathcal{O}(N^2)$, offering significant computational savings. While still less efficient than the Fast Fourier Transform (FFT), which operates with a complexity of $\mathcal{O}(N \log N)$, the MMT approach remains well-suited for medium-sized problems [BY11, VBL⁺16]. It is also worth emphasizing that in our complexity comparison we do not account for the initial cost of precomputing the Clebsch-Gordon coefficients or the matrix coefficients required for the MMT method.*

The primary motivation for the validated MMT approach is to solve nonlinear PDEs using computer-assisted proofs. This work is particularly motivated by the study of the three-dimensional axisymmetric Navier–Stokes equations [Lop94, LS98, HL08, Hou23]. The axisymmetric assumption reduces the problem to a non-local two-dimensional PDE, dependent on the radial variable r and the height variable z . However, applying current CAP techniques to these complex PDEs presents three main challenges. First, the PDEs involve a cylindrical Laplacian, requiring a specialized spectral basis for expansion in the radial variable [AK19]. Second, the equation contains a singular $1/r$ term within the nonlinearities. Lastly, the nonlinearities involve derivatives, further complicating the analysis. These challenges provide a strong motivation for employing the validated MMT approach, which offers a means to overcome these obstacles and provide rigorous solutions.

Our approach to tackling these difficulties involves using orthogonal polynomials defined on the disk, which necessitates the validated MMT approach derived in Section 2. In Section 4, we focus on the special case of Zernike polynomials, which are orthogonal polynomials on the unit disk. In particular, we review their fundamental properties and formulae for linear operators expressed in this basis, which solves the difficulties above in principle. Additionally, we detail how to compute products in the Zernike basis using the MMT, with the computations made rigorous via interval arithmetic, as detailed in Section 3.

To demonstrate the applicability of our approach, we analyze in Section 5 some toy problems on the unit disk $\mathbb{D} \stackrel{\text{def}}{=} \{z \in \mathbb{C}, |z| \leq 1\}$ having quadratic nonlinearities. In particular, given some $m \in \mathbb{N}_0 = \{0, 1, 2, \dots\}$, we study the following complex valued PDE:

$$\begin{cases} \Delta v(z) + \bar{z}^m v(z)^2 = 0, & \text{for all } z \in \mathbb{D} \\ v(e^{i\theta}) = 0, & \text{for all } \theta \in (0, 2\pi). \end{cases} \quad (4)$$

Additionally we consider the following boundary value problem possessing the singular term z^{-1} .

$$\begin{cases} \Delta v(z) + z^{-1} v(z)^2 = 0, & \text{for all } z \in \mathbb{D} \\ v(e^{i\theta}) = 0, & \text{for all } \theta \in (0, 2\pi). \end{cases} \quad (5)$$

The singular inhomogeneous term z^{-1} is meant to be a toy model version of similar terms which appear in the axisymmetric Navier–Stokes equations [HL08, MB02]. In Theorem 5.7, we prove the existence of solution to (4) (for $m = 0, 1, 2, 20$) and (5) (e.g. see Figure 2).

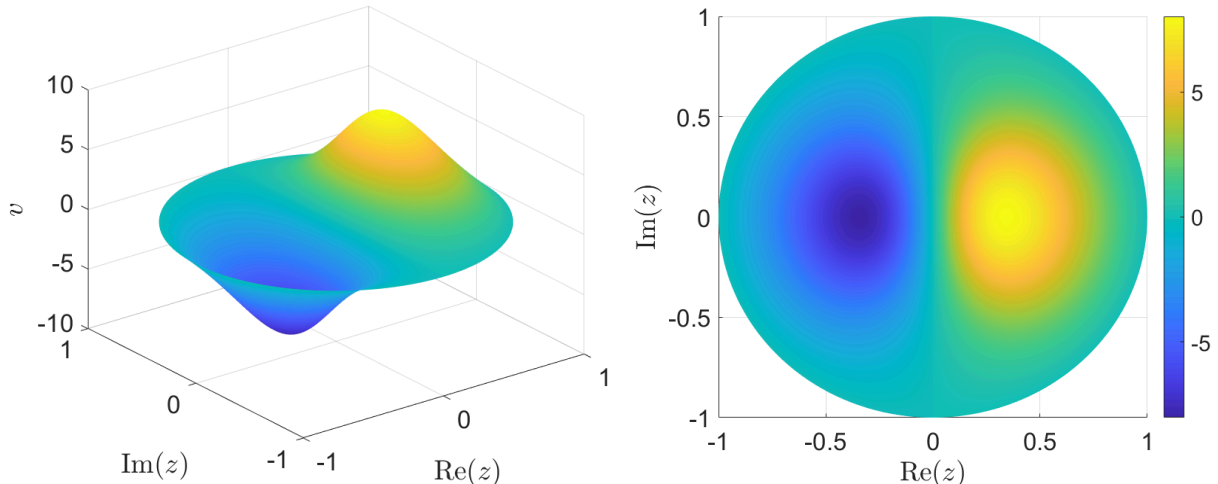


Figure 2: Real part of a numerically computed approximate solution to (5).

In future work we plan to extend this approach to the axisymmetric Navier–Stokes equations. This extension will require addressing the challenges posed by derivatives in the nonlinear terms arising from cylindrical geometry. By leveraging the validated MMT framework, we aim to rigorously analyze these equations and provide a robust foundation for solving complex fluid dynamics problems with axisymmetric assumptions.

2 Orthogonal polynomials and the MMT approach

As discussed earlier in Section 1, the choice of grid points, $\{x_j\}_{j=0}^N$, and polynomials, $\{p_n(x)\}_{n=0}^N$, is crucial for preventing the formation of ill-conditioned MMT matrices. Therefore, making informed selections for these components is essential. A common method involves choosing polynomials p_0, \dots, p_N that are orthogonal with respect to an appropriately defined inner product, with the grid points x_0, \dots, x_N corresponding to the zeros of the polynomial p_{N+1} . In the present section, we outline a general framework for this approach and provide explicit formulas for the entries of the iMMT matrix, along with practical methods for computing these entries. To establish these concepts, we review key elements of orthogonal polynomial theory, Gaussian quadrature and numerical analysis.

2.1 Background on orthogonal polynomials and Gaussian quadrature

Let $\{p_n\}_{n=0}^\infty$ be a sequence of real-valued polynomial such that the degree of $p_n(x)$ is exactly n , that is $p_n(x) = k_n x^n + \mathcal{O}(x^{n-1})$, where $k_n \neq 0$ is called the leading coefficient of p_n . Given an open interval (a, b) ($-\infty \leq a < b \leq \infty$), let $\omega(x)$ be a generic weight function such that

$$\omega(x) > 0, \text{ for all } x \in (a, b) \quad \text{and} \quad \omega \in L^1(a, b).$$

We say that two functions f and g are orthogonal with respect to ω if their inner product $(f, g)_\omega$ satisfies

$$(f, g)_\omega \stackrel{\text{def}}{=} \int_a^b f(x)g(x)\omega(x)dx = 0.$$

Moreover, a sequence of polynomials $\{p_n\}_{n=0}^{\infty}$ is said to be orthogonal with respect to ω if

$$(p_n, p_m)_\omega = \int_a^b p_n(x)p_m(x)\omega(x)dx = \begin{cases} 0, & m \neq n, \\ W_n, & m = n, \end{cases} \quad (6)$$

where

$$W_n \stackrel{\text{def}}{=} \|p_n\|_\omega^2 = \int_a^b p_n(x)^2\omega(x)dx \quad (7)$$

is a nonzero constant. If $W_n = 1$ for all n , then the polynomials are said to be *orthonormal*. Otherwise, these are called *orthogonal polynomials* (with the weight function ω).

A standard result (e.g. see Corollary 3.1 in [STW11]) states that for a given weight function $\omega(x)$, there exists a unique sequence of orthogonal polynomials $\{p_n\}_{n=0}^{\infty}$ with leading coefficients k_n , given by the three-term recurrence relation

$$p_{n+1} = (\alpha_n x - \beta_n)p_n - \gamma_n p_{n-1}, \quad n \geq 0 \quad (8)$$

with $p_{-1} = 0$, $p_0 = k_0$, and with

$$\alpha_n \stackrel{\text{def}}{=} \frac{k_{n+1}}{k_n}, \quad \beta_n \stackrel{\text{def}}{=} \frac{k_{n+1}}{k_n} \frac{(xp_n, p_n)_\omega}{\|p_n\|_\omega^2} \quad \text{and} \quad \gamma_n \stackrel{\text{def}}{=} \frac{k_{n-1}k_{n+1}}{k_n^2} \frac{\|p_n\|_\omega^2}{\|p_{n-1}\|_\omega^2}. \quad (9)$$

Jacobi polynomials form a significant and extensive class of orthogonal polynomials, playing a central role in the applications we propose in this paper. We now proceed to introduce them.

Definition 2.1 (Jacobi polynomials). *Given numbers $k, m > -1$ and the weight $\omega(x) \stackrel{\text{def}}{=} (1-x)^k(1+x)^m$ (sometimes we simply refer to the weight as the pair (k, m)), the Jacobi polynomials $P_n^{k,m}(x)$ defined in $(-1, 1)$ are orthogonal with respect to ω , and they satisfy the recurrence formula $P_{n+1}^{k,m}(x) = (\alpha_n x - \beta_n)P_n^{k,m}(x) - \gamma_n P_{n-1}^{k,m}(x)$, for $n \geq 0$, with $P_{-1}^{k,m}(x) = 0$ and $P_0^{k,m}(x) = 1$, where we have*

$$\alpha_n = \frac{(2n+k+m+1)(2n+k+m+2)}{2(n+1)(n+k+m+1)}, \quad \beta_n = \frac{(m^2-k^2)(2n+k+m+1)}{2(n+1)(n+k+m+1)(2n+k+m)}, \quad \gamma_n = \frac{(n+k)(n+m)(2n+k+m+2)}{(n+1)(n+k+m+1)(2n+k+m)}.$$

When the polynomials p_n are orthogonal as in (6), the coefficients a_n in (1) can be obtained by taking the inner product (\cdot, p_n) on both sides of (1). This yields the expression

$$a_n = \frac{(f, p_n)_\omega}{W_n}, \quad n = 0, \dots, N,$$

which can be challenging to evaluate analytically for functions f with intricate forms. However, if f is a polynomial, Gaussian quadrature provides an efficient method for computing the inner product explicitly. To formalize this approach, let $\{x_j\}_{j=0}^N$ be the zeros of the orthogonal polynomial p_{N+1} with respect to the weight function ω and let $\{\omega_j\}_{j=0}^N$ be the weights defined by

$$\omega_j \stackrel{\text{def}}{=} \int_a^b h_j(x)\omega(x)dx, \quad (10)$$

where the $h_j(x)$ are the standard Lagrange basis polynomials. Then (e.g. see Theorem 3.5 in [STW11] or Theorem 14 of Sec. 4.3 in [Boy01]), the quadrature formula

$$\int_a^b f(x)\omega(x)dx = \sum_{0 \leq j \leq N} f(x_j)\omega_j \quad (11)$$

holds for any f being a polynomial of degree at most $2N + 1$.

The following result (e.g. see Theorem 18 of Sec. 4.4 in [Boy01]), which directly follows from (11), will enable us to derive an explicit formula for the entries of the iMMT matrix when f is a polynomial.

Theorem 2.2 (iMMT matrix via Gaussian quadrature). *Let $\{p_n(x)\}_{n=0}^{\infty}$ be a sequence of orthogonal polynomials with respect to a weight function $w(x)$ on the interval $[a, b]$ and let $\{x_j\}_{j=0}^N$ be the $N + 1$ distinct roots of the orthogonal polynomial $p_{N+1}(x)$. Then, any polynomial $f(x)$ of degree at most N can be uniquely represented in the orthogonal polynomial basis as in (1), where the coefficients a_n are given by*

$$a_n = \frac{(f, p_n)_\omega}{W_n} = \frac{1}{W_n} \int_a^b f(x) p_n(x) \omega(x) dx = \sum_{j=0}^N \frac{\omega_j p_n(x_j)}{W_n} f(x_j), \quad n = 0, \dots, N.$$

Hence, each entry of the iMMT matrix M^{-1} is defined as

$$(M^{-1})_{n,j} \stackrel{\text{def}}{=} \frac{\omega_j p_n(x_j)}{W_n}, \quad (12)$$

where n represents the row index and j represents the column index of B .

In summary, to compute the entries of the iMMT matrix given in (12) and the MMT matrix defined in (3), it is essential to determine several key components, specifically:

- $\{x_j\}_{j=0}^N$: the nodes (roots of p_{N+1})
 - $\{\omega_j\}_{j=0}^N$: the weights in the Gaussian quadrature in (10)
 - $p_n(x_j)$: the values of the orthogonal polynomials at the nodes via (8)
 - W_n : the scaling factors in (7).
- (13)

We explain in the next section details how to perform each these computations rigorously and provide some explicit formulas in the context of Jacobi polynomials (e.g. see Definition 2.1).

2.2 Computing the entries of the MMT and iMMT matrices

To outline a framework for rigorously computing the entries of the MMT matrix M defined in (3) and the iMMT matrix M^{-1} defined in (12), it is essential to rigorously compute all the quantities specified in (13). We proceed as follows: in Section 2.2.1, we explain how to obtain the nodes x_j by calculating the eigenvalues of a specific symmetric tridiagonal matrix \mathcal{A}_{N+1} , as defined in (14). In Section 2.2.2, we show how to determine the weights ω_j using the eigenvectors of \mathcal{A}_{N+1} . Section 2.2.3, introduces two methods for evaluating the orthogonal polynomials at the grid points $p_n(x_j)$: one utilizing the recurrence relation (8), and the other involving the solution of a linear system. In Section 2.2.4, we provide a brief discussion on deriving the formula for the scaling factor W_n and present the explicit expression within the framework of Jacobi polynomials. It is important to note that these computations are inherently susceptible to rounding errors. Given that our goal is to produce computer-assisted proofs of the existence of solutions to PDEs, we must establish rigorous and efficient methods for controlling all errors in evaluating the quantities listed in (13), which are crucial for accurately constructing the matrices M and M^{-1} . This subject is thoroughly discussed in Section 3.

2.2.1 Computing the nodes x_j

We start by describing how to obtain the nodes $\{x_j\}_{j=0}^N$, which, it is important to recall, are the zeros of the orthogonal polynomial p_{N+1} . These nodes are crucial because they are also used to generate computational grids for spectral methods. While methods like Newton's algorithm could be employed to find the zeros of p_{N+1} , we present the more efficient *Golub-Welsch algorithm* [GW69], which is specifically designed to compute the zeros of orthogonal polynomials accurately.

Recalling the coefficients α_n , β_n and γ_n be defined as in (9), it is known (e.g. see Theorem 3.4 in [STW11]) that the zeros $\{x_j\}_{j=0}^N$ of the orthogonal polynomial p_{N+1} are the eigenvalues of the following symmetric tridiagonal matrix

$$\mathcal{A}_{N+1} = \begin{pmatrix} \mu_0 & \eta_1 & & & \\ \eta_1 & \mu_1 & \eta_2 & & \\ & \ddots & \ddots & \ddots & \\ & & \eta_{N-1} & \mu_{N-1} & \eta_N \\ & & & \eta_N & \mu_N \end{pmatrix} \quad (14)$$

where $\mu_j = \frac{\beta_j}{\alpha_j}$ for $j \geq 0$ and $\eta_j = \frac{1}{\alpha_{j-1}} \sqrt{\frac{\alpha_{j-1}\gamma_j}{\alpha_j}}$ for $j \geq 1$. The computation of an eigenvalue-eigenvector pair (λ, u) of \mathcal{A}_{N+1} such that $\|u\|^2 = 1$ can be reformulated as looking for a solution of the

$$F^{\text{eig}}(\lambda, u) \stackrel{\text{def}}{=} \begin{pmatrix} (u, u)_2 - 1 \\ \mathcal{A}_{N+1}u - \lambda u \end{pmatrix}. \quad (15)$$

In Section 3, we present a Newton-Kantorovich theorem (see Theorem 3.1) that, when combined with interval arithmetic, can be used to rigorously determine the locations of all eigenvalue-eigenvector pairs of \mathcal{A}_{N+1} by solving problem (15) $N + 1$ times.

2.2.2 Computing the weights ω_j

With a strategy in place for computing the nodes x_j , the next step is to calculate the weights ω_j defined in (11). Let $Q(x_j) = (Q_0(x_j), \dots, Q_N(x_j))^T \in \mathbb{R}^{N+1}$ be an eigenvector of \mathcal{A}_{N+1} associated with the eigenvalue x_j such that $\|Q(x_j)\|^2 = (Q(x_j), Q(x_j))_2 = 1$. According to Theorem 3.6 in [STW11], the weights $\{\omega_j\}_{j=0}^N$ can be obtained from the first component of the eigenvector $Q(x_j)$ using the formula

$$\omega_j = [Q_0(x_j)]^2 \int_a^b \omega(x) dx. \quad (16)$$

Remark 2.3 (Computing the weights for Jacobi polynomials). *In case we are working with Jacobi polynomials, which are orthogonal with respect to the weight $\omega(x) = (1-x)^k(1+x)^m$ with $k, m \in \mathbb{N}_0$, Equation (3.144) from [STW11] yields the explicit expression*

$$\int_a^b \omega(x) dx = \int_{-1}^1 (1-x)^k(1+x)^m dx = \frac{2^{k+m+1}k!m!}{(k+m+1)!}.$$

For Jacobi polynomials, the only remaining task to compute ω_j in (16) is to compute the value $Q_0(x_j)$, which is obtained by computing the eigenvectors of the matrix \mathcal{A}_{N+1} defined in (14).

2.2.3 Evaluating $p_n(x_j)$: the orthogonal polynomials at the grid points

In this section, we present three distinct methods for evaluating $p_n(x_j)$ for $j, n = 0, \dots, N$, which correspond to the values of orthogonal polynomials at the grid points. These methods include: the Forsythe algorithm, which utilizes the recurrence relation; a linear system approach, solved using a Newton-Kantorovich method with an approximate inverse; and a technique based on the eigenvectors of the matrix \mathcal{A}_{N+1} .

Method 1 (Forsythe algorithm). Recalling the recurrence formula given in (8), a first approach to computing the values $p_n(x_j)$ is to use the previously obtained nodes x_j , by setting $p_{-1} = 0$ and $p_0 = k_0$ and then directly evaluating

$$p_{n+1}(x_j) = (\alpha_n x_j - \beta_n) p_n(x_j) - \gamma_n p_{n-1}(x_j), \quad n \geq 0.$$

This method, called the *Forsythe algorithm* [For57], is commonly used in practice. However, it is well known that numerical stability can be a concern when computing recurrence relations, particularly when using interval arithmetic, leading to potential accuracy issues. To mitigate this, two approaches can be employed: using high-precision arithmetic or solving a linear system (see (17) below) derived from the recurrence relation (referred to as the *linear system approach*). In Section 3, we implement Methods 1 and 2 alongside interval arithmetic and compare their performance in Section 3.1. Before doing so, let us provide further details on our implementation of the linear system approach.

Method 2 (Linear System Approach). For a fixed $x \in (a, b)$, rewriting (8) into a matrix form

$$\mathbf{A}(x)\mathbf{p}(x) = \mathbf{e}_1, \tag{17}$$

where $\mathbf{A}(x) \in \mathbb{R}^{(N+1) \times (N+1)}$ and $\mathbf{p}(x), \mathbf{e}_1 \in \mathbb{R}^{N+1}$ are defined by

$$\mathbf{A}(x) \stackrel{\text{def}}{=} \begin{pmatrix} 1 & & & & \\ \vartheta_0(x) & 1 & \ddots & \ddots & \\ \gamma_1 & \vartheta_1(x) & 1 & \ddots & \\ & & & \ddots & \\ & & & \gamma_{N-1} & \vartheta_{N-1}(x) & 1 \end{pmatrix}, \quad \vartheta_n(x) \stackrel{\text{def}}{=} -(\alpha_n x - \beta_n), \tag{18}$$

and

$$\mathbf{p}(x) \stackrel{\text{def}}{=} (p_0(x), p_1(x), \dots, p_N(x))^T, \quad \mathbf{e}_1 \stackrel{\text{def}}{=} (1, \dots, 0, 0)^T,$$

respectively. Then, setting $x = x_j$ for $j = 0, \dots, N$ in (18), the solution of the linear system $\mathbf{p}(x_j) = \mathbf{A}(x_j)^{-1} \mathbf{e}_1$ gives the j -th column of the MMT matrix M , that is the value of the orthogonal polynomials at the grid points $p_n(x_j)$. To obtain a rigorous enclosure of the solution to $\mathbf{A}(x_j)\mathbf{p}(x_j) = \mathbf{e}_1$, we can use the Newton-Kantorovich Theorem 3.1 in conjunction with interval arithmetic to rigorously determine the location of the solution to the system defined by

$$F^{x_j}(p) \stackrel{\text{def}}{=} \mathbf{A}(x_j)p - \mathbf{e}_1. \tag{19}$$

We refer to this way of evaluating the orthogonal polynomials at the grid points, that is $p_n(x_j)$, as the *linear system approach*. Although this approach may initially seem excessive for solving a linear system, the Newton-Kantorovich Theorem requires only an approximate inverse, which can

be computed without interval arithmetic, thereby minimizing the wrapping effect. This is further explained in Section 3.

The third approach (e.g. see [GW69]) we introduce for evaluating the orthogonal polynomials at the grid points utilizes the eigenvectors of \mathcal{A}_{N+1} .

Method 3 (via the eigenvectors of \mathcal{A}_{N+1}). The matrix \mathcal{A}_{N+1} is derived from the similarity transformation $\mathcal{A}_{N+1} = DJD^{-1}$. Here, J is the following non-symmetric tridiagonal matrix, called the *Jacobi matrix*:

$$J = \begin{pmatrix} \beta_0/\alpha_0 & 1/\alpha_0 & & & & \\ \gamma_1/\alpha_1 & \beta_1/\alpha_1 & & 1/\alpha_1 & & \\ & \ddots & & \ddots & & \ddots \\ & & & \gamma_{n-1}/\alpha_{n-1} & \beta_{n-1}/\alpha_{n-1} & 1/\alpha_{n-1} \\ & & & & \gamma_n/\alpha_n & \beta_n/\alpha_n \end{pmatrix}, \quad (20)$$

where α_n , β_n , and γ_n are the coefficients in the recurrence formula given in (9) satisfying the three-term recurrence formula (8). The diagonal similarity transformation is performed via the matrix D given by

$$D = \begin{pmatrix} d_0 & & & & \\ & d_1 & & & \\ & & \ddots & & \\ & & & \ddots & \\ & & & & d_n \end{pmatrix}, \quad d_{i+1} = \sqrt{\frac{\alpha_{i+1}}{\alpha_i \gamma_{i+1}}} d_i \quad (d_0 = 1). \quad (21)$$

Considering an eigenpair $(x_j, Q(x_j))$ satisfying $\mathcal{A}_{N+1}Q(x_j) = x_jQ(x_j)$, then from the similarity transformation $\mathcal{A}_{N+1} = DJD^{-1}$ given in (20) and (21), it follows that

$$DJJ^{-1}Q(x_j) = x_jQ(x_j) \iff JD^{-1}Q(x_j) = x_jD^{-1}Q(x_j).$$

Here, the eigenvalues of J are the same as that of \mathcal{A}_{N+1} . Since the matrix J directly comes from the recurrence formula (8), eigenvectors of J , that is $D^{-1}Q(x_j)$, are equal to the values of the orthogonal polynomial, i.e., $(p_n(x_j))_{n=0}^N$, except for the scaling freedom. To fix the scale satisfying $p_0 = k_0$, we have

$$p_n(x_j) = \frac{(D^{-1}Q(x_j))_n}{(D^{-1}Q(x_j))_0} k_0, \quad (22)$$

where $(D^{-1}Q(x_j))_n$ denotes the n -th component of the vector $D^{-1}Q(x_j)$. Formula (22) is yet another method to evaluating the orthogonal polynomials at the grid points, hence providing a way to compute the entries of the MMT matrix M defined in (3).

2.2.4 Computing the scaling factors W_n

Deriving analytic expressions for the scaling factors W_n defined in (7) for different families of orthogonal polynomials is a well-established area of study with a rich history. Various tables, such as those found in [GR00], provide these expressions for many significant families, including Legendre, Chebyshev, Hermite, and Laguerre polynomials. For the Jacobi polynomials $P_n^{k,m}$ with k and m non negative integers, it is given by

$$W_n = W_n^{k,m} = \frac{2^{k+m+1}}{2n+k+m+1} \frac{(n+k)!(n+m)!}{(n+k+m+1)!n!}.$$

For non-integer values of $k, m > -1$, this formula extends to the use of Gamma functions. Additionally, for validated numerical computations, it is crucial to handle cancellations carefully when dividing factorials by other factorials — e.g. $\frac{(n+k)!(n+m)!}{(n+k+m+1)!n!} = \frac{\prod_{i=1}^k (n+i)}{\prod_{i=1}^{k+1} (n+m+i)}$ — to avoid a significant increase in round-off errors.

3 Validated numerics and comparisons

The discussion of Section 2 has been a review of standard orthogonal polynomials, Gaussian quadrature and numerical analysis concepts. While Gaussian quadrature is theoretically exact when using the correct nodes x_j and weights ω_j , this requires an accurate calculation of these nodes and weights, as well as their evaluation under the relevant polynomials. However, computers use floating point arithmetic, which operates with finite precision. In numerical quadrature, the primary challenge to achieving accuracy often stems from rounding errors and the limitations of finite precision arithmetic [Bar02, HT13, Bog14].

As numerical quadrature serves as the foundation for subsequent computations, any imprecision introduced here will propagate. At a fundamental level, if a node is computed with machine precision, $x_i = \bar{x}_i \pm 10^{-16}$, the error in its evaluation under a function f will be at least $|f(x_i) - f(\bar{x}_i)| \approx |f'(x_i)| \times 10^{-16}$. For Legendre polynomials, their derivative at the endpoint is given by $P'_n(1) = \frac{n(n+1)}{2}$. Hence, for a truncation at $N = 100$, the error could be amplified by four orders of magnitude. A more accurate calculation of $f(x_i)$ can be achieved by computing x_i with multiple precision. While precision will still be lost when evaluating $f(x_i)$, starting with higher precision ensures that the final result is sufficiently accurate. However, using multiple precision requires more memory and is slower compared to double precision.

To synthesize the various types of errors encountered in numerical computations, we employ validated numerics [Tuc11, Rum10, Nak01, KSW96, vdBL15]. A fundamental aspect of validated numerics is interval arithmetic, which rigorously bounds rounding errors. This approach allows us to derive explicit *a posteriori* error bounds for our results. Although limited work has been done in the area of Gaussian quadrature using validated numerics [Sto93], these methods enable us to set specific accuracy goals; for instance, we may aim for the entries of the MMT/iMMT matrices M and M^{-1} to achieve an accuracy of 10^{-16} . While obtaining the nodes with high (and therefore slower) precision may be necessary, we can subsequently store the computed matrices M and M^{-1} as a double matrix.

Recall from Sections 2.2.1 and 2.2.2 that computing the nodes $\{x_j\}_{j=0}^N$ and weights $\{\omega_j\}_{j=0}^N$ first requires determining all eigenpairs of the matrix \mathcal{A}_{N+1} defined in (14). We interpret each eigenpair as a zero of the map specified in (15). Furthermore, as described in Section 2.2.3, Method 2 for evaluating $p_n(x_j)$ involves selecting a grid point x_j and finding the zero of the map given in (19). To solve these two zero-finding problems, we apply a Newton-Kantorovich theorem that rigorously encloses the zeros, presented below in a general setting for maps between Banach spaces. This theorem offers rigorous *a posteriori* estimates for locating zeros of a function. Moreover, we will use this theorem to establish the existence of solutions to elliptic semilinear PDEs on the disk, as detailed in Section 5.

Theorem 3.1 (Newton-Kantorovich Theorem). *Let X and X' be Banach spaces and $F : X \rightarrow X'$ be a Fréchet differentiable mapping. Suppose $x_0 \in X$ and $A \in B(X', X)$. Moreover assume that A is injective. Let Y_0 and Z_1 be positive constants and $Z_2 : (0, \infty) \rightarrow [0, \infty)$ be a non-negative*

function satisfying

$$\begin{aligned} \|AF(x_0)\|_X &\leq Y_0, \\ \|I - ADF(x_0)\|_{B(X)} &\leq Z_1, \\ \|A[DF(c) - DF(x_0)]\|_{B(X)} &\leq Z_2(r)r, \quad \text{for all } c \in \overline{B_r(x_0)} \text{ and all } r > 0. \end{aligned}$$

Define

$$p(r) = Z_2(r)r^2 - (1 - Z_1)r + Y_0.$$

If there exists $r_0 > 0$ such that $p(r_0) < 0$, then there exists a unique $\tilde{x} \in \overline{B_{r_0}(x_0)}$ satisfying $F(\tilde{x}) = 0$.

Typically, the vector x_0 is a numerical approximation, while the operator A serves as an approximate inverse of the derivative $DF(x_0)$.

3.1 Comparison: Evaluation of the Jacobi Polynomials

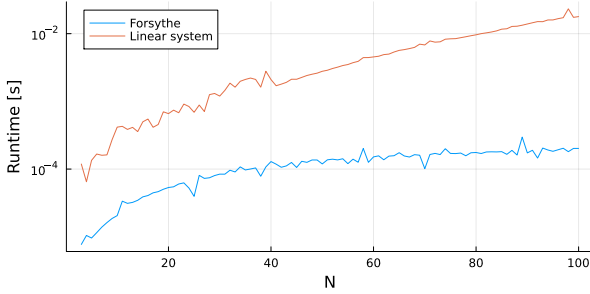
We now turn to the evaluation of Jacobi polynomials as introduced in Definition 2.1. Specifically, we consider the case $k = m = 1$ and analyze the performance of the first two methods described in Section 2.2.3: the Forsythe algorithm and the linear system approach, which employs Theorem 3.1 to determine the zeros of the map (19). We compare these methods under a fixed working precision, focusing on both runtime performance (illustrated in Figure 3a) and the error associated with the evaluation of the Jacobi polynomials (shown in Figure 3b). For the runtime assessment, we varied the degree N of the Jacobi polynomial and computed $P_N^{k,m}$ at a random point in $[-1, 1]$.

As depicted in Figure 3a, Forsythe algorithm significantly outperforms the linear system approach in terms of runtime, owing to its computational complexity of $\mathcal{O}(N)$ compared to the $\mathcal{O}(N^3)$ complexity of the linear system approach. However, as illustrated in Figure 3b, the interval radii produced by Forsythe algorithm exhibit much greater instability. In contrast, while the interval radii for the linear system approach also increase with N , they are more controlled. This discrepancy arises from the inherent wrapping effect associated with recursion-based algorithms, for which interval arithmetic is particularly ill-suited. Additionally, for both methods, the output interval radii are insufficient to achieve 10^{-16} accuracy for the MMT matrix M defined in (3). This limitation stems from the large magnitudes of polynomial values as N increases. Therefore, employing higher precision in numerical computations may be necessary.

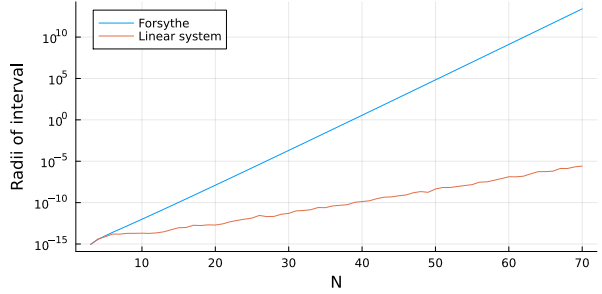
We now examine the necessary working precision to ensure that the evaluation of $P_N^{k,m}(x)$ attains machine precision for 64-bit floating-point numbers (approximately $\approx 10^{-16}$ accuracy). The implementation is based on the Julia programming language [BEKS17], utilizing the `BigFloat` type in conjunction with the `IntervalArithmetic.jl` package [SB14]. The precision of `BigFloat` numbers is controlled by the `setprecision` function, which adjusts the number of significant bits in the floating-point representation¹.

We selected several random points $x \in [-1, 1]$ and adjusted varied the precision of `BigFloat` to obtain accurate results for the polynomial evaluations. In Figure 4a, we present the required precision for each degree N to ensure that the output radius of the interval inclusion is below the machine precision. It is observed that the Forsythe algorithm, which uses recursive formulas, demands significantly higher precision compared to the linear system approach. However, the linear system approach still requires high precision to achieve machine precision, albeit to a lesser extent than the Forsythe algorithm.

¹More specifically, `setprecision` sets the “number of bits for significant + 1”, as defined in the Julia language.

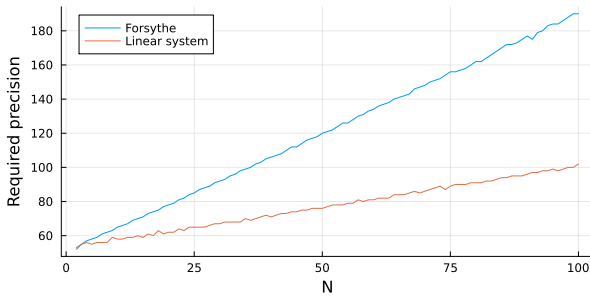


(a) The plot illustrates the runtime (in seconds) as a function of the polynomial degree N for evaluating $P_N^{1,1}(x)$ at a random point $x \in [-1, 1]$ using interval arithmetic. It is evident that the Forsythe algorithm is significantly faster than the linear system approach.

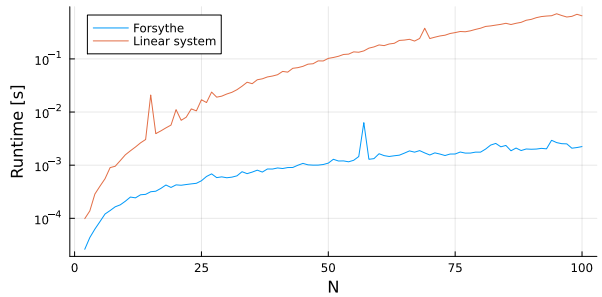


(b) The relationship between the polynomial degree N and the maximum radius of the output interval inclusions for evaluating $P_N^{1,1}$ at 50 random points within $[-1, 1]$ is shown. We observe that the error bounds for the Forsythe algorithm increase rapidly, primarily due to the wrapping effect that arises when using interval arithmetic for the recursion formula.

Figure 3: Comparison of evaluating $P_n^{1,1}$ with interval arithmetic via Forsythe algorithm and the linear system approach in terms of (a) running time and (b) resulting error in evaluations.



(a) In the plot, we illustrate the precision of the arithmetic (as a function of N required to ensure that the output radius of the interval inclusion of $P_N^{1,1}(x)$ is below the machine precision ϵ for 64-bit floating-point numbers. It is observed that both algorithms require more than N -precision (which corresponds to high-precision arithmetic when $N > 64$ to achieve the machine precision ϵ).



(b) The runtime (as a function of the polynomial order N) for each algorithm (Forsythe and linear system approach) when evaluating the polynomial $P_N^{1,1}(x)$ with the necessary high-precision arithmetic (depicted in the left figure) to achieve the machine precision ϵ . The plot reveals that the Forsythe algorithm requires less time for evaluation, despite needing higher precision numbers.

Figure 4: Comparison of each algorithm in terms of (a) required precision to achieve the output accuracy below machine precision and (b) running time with the required precision. Forsythe algorithm is the appropriate choice if arbitrary precision floating-point numbers are available.

In addition, Figure 4b illustrates the runtime for evaluating the polynomial with the required precision for each algorithm. Despite the Forsythe algorithm requiring higher precision, it is computationally more efficient and results in faster evaluation times compared to the linear system approach.

From these observations, we conclude that Forsythe algorithm is the preferred method when arbitrary-precision floating-point numbers are available. This conclusion follows from the computational complexity differences between the algorithms, as well as the capabilities of the Julia environment, where the computation of arbitrary-precision numbers is not prohibitively expensive.

sive. Conversely, in environments where interval arithmetic with arbitrary-precision numbers is not supported, the linear system approach is likely to be the more favorable choice.

4 Zernike Polynomials

Chebyshev and Legendre polynomials are among the most commonly used orthogonal polynomials on $[-1, 1]$, corresponding to specific cases of Jacobi Polynomials (cf. Definition 2.1) with weights $(-1/2, -1/2)$ and $(0, 0)$. Other weights (k, m) commonly arise when making a change of coordinates to $[-1, 1]$ from another geometry, e.g., spherical or polar coordinates. Such is the case for defining a function basis on the disk $\mathbb{D} = \{x^2 + y^2 \leq 1\}$, where typically one takes a polar-radial function basis

$$f(\theta, r) = \sum_{m=0}^{\infty} (a_m \cos m\theta + b_m \sin m\theta) p_m(r), \quad p_m(r) = \sum_n c_{m,n} p_{m,n}(r)$$

for $\theta \in [0, 2\pi]$, $r \in [0, 1]$, and some basis of radial basis functions $p_{m,n} : [0, 1] \rightarrow \mathbb{R}$.

There are numerous ways to define the basis functions $p_{m,n}$, each with its own advantages and disadvantages, as discussed in [BY11]. A key consideration in this context is the so-called pole condition at $r = 0$. Specifically, for a function f to be smooth at $r = 0$, the basis function $p_m(r)$ must possess a zero of order m at $r = 0$. This condition can either be imposed numerically or inherently satisfied by selecting appropriate basis functions $p_{m,n}$ that naturally fulfill this requirement.

There is no universal “best” basis for radial functions. While Bessel functions form an eigenbasis for the Dirichlet Laplacian on the disk, their product is generically an infinite series of other Bessel functions, which lacks desirable approximation properties. A commonly used basis for radial functions is given by rescaled Chebyshev functions, which allow efficient evaluation of nonlinearities using the FFT in both variables. Additionally, smooth functions have rapidly converging Chebyshev expansions in this basis. However, this basis does not inherently satisfy the pole condition, and the pseudo-differential operator arising from the Galerkin truncation leads to heptadiagonal matrices, i.e., banded matrices of width seven, as discussed in the works of Boyd [BY11] and Shen [She00].

An effective compromise is provided by the *Zernike polynomials*, also known as *disk polynomials* or *one-sided Jacobi polynomials* and are defined on the unit disk. Zernike polynomials [Zer34, BW99, Nol76] are a sequence of orthogonal polynomials with respect to the natural L^2 inner product on the disk, similar to the Legendre polynomials, and possess favorable approximation properties. Named after Frits Zernike, the optical physicist who received the 1953 Nobel Prize in Physics for inventing phase-contrast microscopy, these polynomials are widely used in optics, image analysis, and wavefront fitting. They are particularly useful in describing wavefront aberrations in circular apertures, such as lenses or mirrors in optical systems. Additionally, the natural differential operators on the disk induce relatively simple pseudo-differential operations on the coefficients of the Zernike polynomials. This is analogous to the situation with Chebyshev polynomials of the first kind, where derivatives are most efficiently expressed in terms of Chebyshev polynomials of the second kind, as demonstrated by the identity $\frac{d}{dx} T_n(x) = nU_{n-1}(x)$. Similarly, an analogous relationship exists for the derivatives of Zernike polynomials.

In the rest of this section, we define formally the Zernike polynomials, demonstrate that the function space of Zernike series polynomials forms a Banach algebra, and apply the MMT approach outlined in Section 2 to the multiplication of Zernike polynomials. Evaluating nonlinearities in a Zernike polynomial basis is computationally more expensive than in a Chebyshev polynomial basis, primarily due to the lack of an FFT-like algorithm for Zernike polynomials. However, our MMT approach achieves a computational complexity of $\mathcal{O}(N^2)$ with respect to the polynomial degree, as noted in Remark 1.2.

4.1 Definition of the Zernike polynomials

As there is not a universally agreed upon notation for Zernike polynomials (e.g. see [Koo78, Kan85, MM95a, BY11, VBL⁺16, AK19]), we now fix our own notation.

Definition 4.1 (Zernike polynomials). *For each $k > -1$, and azimuthal wave number $m \in \mathbb{Z}$, we define the n^{th} Zernike polynomial $\mathcal{Q}_n^{k,m}$ with weight (k, m) as*

$$\mathcal{Q}_n^{k,m}(r, \theta) \stackrel{\text{def}}{=} e^{im\theta} Q_n^{k,m}(r), \quad Q_n^{k,m}(r) \stackrel{\text{def}}{=} r^{|m|} P_n^{k,|m|}(x)$$

for $x = 2r^2 - 1$ and Jacobi polynomials $P_n^{k,|m|}(x)$, introduced in Definition 2.1. We also refer to $Q_n^{k,m}(r)$ as the radial Zernike polynomials.

By writing a complex numbers as $z = re^{i\theta}$, we may also interpret $\mathcal{Q}_n^{k,m}$ as being defined on the complex disk, $\mathcal{Q}_n^{k,m} : \mathbb{D} \rightarrow \mathbb{C}$. In this manner we may write general functions $u : \mathbb{D} \rightarrow \mathbb{C}$ as a Zernike polynomials series

$$u(r, \theta) = \sum_{m \in \mathbb{Z}, n \geq 0} u_{m,n} \mathcal{Q}_n^{k,m}(r, \theta) = \sum_{m \in \mathbb{Z}} e^{im\theta} \sum_{n \geq 0} u_{m,n} Q_n^{k,m}(r)$$

which exhibit spectral convergence for analytic functions (e.g. see [Wal65, MM95a, BY11]).

It is common in the literature to define Zernike polynomials as real-valued functions; however, we opt for a complex-valued definition. This choice mirrors the distinction between Fourier series and trigonometric series. The complex formulation proves particularly advantageous when analyzing the expansion of pseudo-differential operators in terms of Zernike polynomials, as discussed in Section 4.4. For all $m \in \mathbb{Z}$ and $z \in \mathbb{D}$, we have the relationship

$$\mathcal{Q}_n^{k,-m}(z) = \overline{\mathcal{Q}_n^{k,m}(z)}. \quad (23)$$

When restricting to real-valued functions $u : \mathbb{D} \rightarrow \mathbb{R}$, the coefficients must satisfy $u_{m,n} = \bar{u}_{-m,n}$. Furthermore, by identifying $\mathbb{C} \cong \mathbb{R}^2$, Zernike polynomials offer an elegant representation for vector fields defined on the disk. This representation is particularly useful for translating a vector-valued PDE into its corresponding spectral formulation.

4.2 Banach Algebra

Having established the Zernike polynomials, we now formalize a Banach space consisting of rapidly decaying Zernike coefficients of functions expressed as series in terms of Zernike polynomials. We will demonstrate that this sequence space forms a Banach algebra under a suitably chosen weighted norm. This structure will be particularly useful for the nonlinear analysis required in the computer-assisted proofs of existence for solutions to elliptic semilinear PDEs on the disk, as discussed in Section 5.

Definition 4.2. *Fix a Banach space X and a product structure $*$: $X \times X \rightarrow X$. Then $(X, *)$ is said to be a Banach algebra if for all $a, b \in X$,*

$$\|a * b\|_X \leq \|a\|_X \|b\|_X.$$

It is well-established that the space of functions represented as series in Zernike polynomials can be endowed with a Banach algebra structure under an appropriate norm [Kan85, AK19]. By choosing a suitably weighted norm, this space can be made to correspond to either real analytic functions or weakly differentiable functions. Below, we provide a definition of admissible weighted norms that yield a Banach algebra, thereby generalizing several results previously established in the literature.

Definition 4.3. We say that a sequence of weights $(w_{m,n})_{(m,n) \in \mathbb{Z} \times \mathbb{N}_0}$ is admissible if:

$$w_{m,n} \geq 1, \quad w_{m,n} \leq w_{m,n+1}$$

and the weights are submultiplicative in the following sense:

$$w_{m_1+m_2, n'} \leq w_{m_1, n_1} w_{m_2, n_2}, \quad n' = n_1 + n_2 + \frac{|m_1| + |m_2| - |m_1 + m_2|}{2}.$$

We note that the radial Zernike polynomials $Q_n^{k,m}(r)$ are polynomials of degree $2n + |m|$, and some possible choices of w which grow geometrically or algebraically are:

$$w_{m,n} = \nu^{2n+|m|}, \quad w_{m,n} = (1 + 2n + |m|)^s$$

for $\nu \geq 1$ or $s \geq 0$. The proof is left to the reader. The geometric weights correspond to analytic functions, whereas the algebraic weights are analogous to a Sobolev norm (e.g. see Definition 4.4).

As we will discuss further in Section 4.4, the index k in the definition of Zernike polynomials is a grading which essentially corresponds to derivatives, similar to Chebyshev polynomials of the first, second, etc kind. If $-1 < k \leq 0$ then all the polynomials $Q_n^{0,m}(r)$ are bounded between -1 and 1 , however in general $\|Q_n^{k,m}\|_{L^\infty}$ grows algebraically in n . In particular for integers $k \geq 0$ we have:

$$\sup_{r \in [0,1]} |Q_n^{k,m}(r)| = Q_n^{k,m}(1) = \binom{k+n}{n}.$$

Other works in the literature commonly normalize the basis elements by this factor. We opt to incorporate it into our norm.

Definition 4.4. Fix an admissible sequence of weights $(w_{m,n})_{(m,n) \in \mathbb{Z} \times \mathbb{N}_0}$, and define the symbol

$$\langle m, n \rangle_{k,w} = w_{m,n} \binom{k+n}{n}.$$

Define the weighted sequence space V^k as

$$V^k \stackrel{\text{def}}{=} \{a = \{a_{m,n}\}_{m \in \mathbb{Z}, n \in \mathbb{N}_0} \subseteq \mathbb{C} : \|a\|_{V^k} < \infty\}, \quad \|a\|_{V^k} \stackrel{\text{def}}{=} \sum_{m \in \mathbb{Z}, n \in \mathbb{N}_0} |a_{m,n}| \langle m, n \rangle_{k,w}.$$

Analogous to the discrete Fourier transform, we may map a given sequence of Zernike coefficients to the corresponding series of Zernike polynomials. Formally, for each $k \in \mathbb{N}_0$, define a transform $\mathcal{M} : V^k \rightarrow C(\mathbb{D}, \mathbb{C})$ given below, where for $a \in V^k$ and $z = re^{i\theta} \in \mathbb{D}$ we define

$$\mathcal{M}[a](z) \stackrel{\text{def}}{=} \sum_{m \in \mathbb{Z}} \sum_{n \in \mathbb{N}_0} a_{m,n} Q_n^{k,m}(z).$$

Similarly, as the Zernike polynomials form a Schauder basis, an inverse transform \mathcal{M}^{-1} may be defined to recover the Zernike coefficients of a function $u : \mathbb{D} \rightarrow \mathbb{C}$, assuming u has sufficient regularity [Wal65, MM95a, VBL⁺16].

Corresponding to the sequence space V^k — and analogous to the Wiener algebra of functions with absolutely convergent Fourier series — let us define a space consisting of functions whose Zernike coefficients are in V^k .

$$\tilde{V}^k = \left\{ u \in L^2(\mathbb{D}, \mathbb{C}) : \mathcal{M}^{-1}(u) \in V^k \right\}, \quad \|u\|_{\tilde{V}^k} = \|\mathcal{M}^{-1}u\|_{V^k}.$$

Note that by definition \tilde{V}^k is isometrically isomorphic with V^k . Furthermore, we have the bound $\|u\|_{C(\mathbb{D},\mathbb{C})} \leq \|u\|_{\tilde{V}^k}$.

In further analogy with the discrete Fourier transform, the product of functions in $C(\mathbb{D},\mathbb{C})$ induces a discrete convolution of their coefficients in V^k .

Definition 4.5. For $a, b \in V^k$, we define a discrete convolution product $*$: $V^k \times V^k \rightarrow V^k$ by

$$a * b = \mathcal{M}^{-1}(\mathcal{M}[a] \cdot \mathcal{M}[b]).$$

We also will consider the subspace $V^{k,m} \subseteq V^k$ obtained by restricting to a single wave number:

$$V^{k,m} \stackrel{\text{def}}{=} \left\{ a \in V^k : a_{m',n} = 0 \text{ whenever } m' \neq m \right\}. \quad (24)$$

As mentioned earlier, the space of Zernike polynomials forms a Banach algebra for an adequately chosen norm. A key element for this proof is the following result on positivity of linearization coefficients:

Lemma 4.6. Fix k and $m_1, m_2 \in \mathbb{Z}$. Then $*$ restricts to a map $*$: $V^{k,m_1} \times V^{k,m_2} \rightarrow V^{k,m_3}$ for $m_3 = m_1 + m_2$. Furthermore, there exist non-negative linearization coefficients $c_{(m_1,n_1),(m_2,n_2)}^{(m_3,n_3)} \geq 0$ for which

$$\mathcal{Q}_{n_1}^{k,m_1}(z) \mathcal{Q}_{n_2}^{k,m_2}(z) = \sum_{n_3} c_{(m_1,n_1),(m_2,n_2)}^{(m_3,n_3)} \mathcal{Q}_{n_3}^{k,m_3}(z),$$

and the linearization coefficients are non-zero only if

$$|n_1 - n_2| - (|m_1| + |m_2|) \leq n_3 \leq n_1 + n_2 + \frac{|m_1| + |m_2| - |m_1 + m_2|}{2}.$$

Proof. This essentially follows from Corollary 5.2 in [Koo78] which yields that the product of two Zernike polynomials may be written as:

$$\mathcal{Q}_{n_1}^{k,m_1}(z) \mathcal{Q}_{n_2}^{k,m_2}(z) = \sum_{n_3} c_{(m_1,n_1),(m_2,n_2)}^{(m_3,n_3)} \mathcal{Q}_{n_3}^{k,m_3}(z),$$

where $m_3 = m_1 + m_2$ and n_3 is subject to the constraint:

$$|2n_1 + |m_1| - (2n_2 + |m_2|)| \leq 2n_3 + |m_3| \leq 2n_1 + |m_1| + 2n_2 + |m_2|.$$

This is equivalent to

$$\left| n_1 - n_2 + \frac{|m_1| - |m_2|}{2} \right| - \frac{|m_1 + m_2|}{2} \leq n_3 \leq n_1 + n_2 + \frac{|m_1| + |m_2| - |m_1 + m_2|}{2},$$

from which, we obtain the desired result. □

Theorem 4.7. The spaces V^k and \tilde{V}^k are Banach algebras.

Proof. We will first show that

$$\|\mathcal{Q}_{n_1}^{k,m_1} \mathcal{Q}_{n_2}^{k,m_2}\|_{\tilde{V}^k} \leq \|\mathcal{Q}_{n_1}^{k,m_1}\|_{\tilde{V}^k} \|\mathcal{Q}_{n_2}^{k,m_2}\|_{\tilde{V}^k} \quad (25)$$

for any $m_1, m_2 \in \mathbb{Z}$ and $n_1, n_2 \in \mathbb{N}_0$. From Lemma 4.6 it follows that we may write the product of two Zernike polynomials as

$$\mathcal{Q}_{n_1}^{k, m_1}(r, \theta) \mathcal{Q}_{n_2}^{k, m_2}(r, \theta) = e^{i(m_1 + m_2)\theta} \sum_{n_3=0}^{n'} c_{(m_1, n_1), (m_2, n_2)}^{(m_3, n_3)} \mathcal{Q}_{n_3}^{k, m_1 + m_2}(r) \quad (26)$$

for $n' = n_1 + n_2 + \frac{|m_1| + |m_2| - |m_1 + m_2|}{2}$ and real linearization coefficients $c_{(m_1, n_1), (m_2, n_2)}^{(m_3, n_3)}$. Note that as $\mathcal{Q}_n^{k, m}(1) = \binom{k+n}{n}$ and the coefficients are non-negative, letting $(r, \theta) = (1, 0)$ in (26) above, it follows that:

$$\binom{k+n_1}{n_1} \binom{k+n_2}{n_2} = \sum_{n_3=0}^{n'} \left| c_{(m_1, n_1), (m_2, n_2)}^{(m_3, n_3)} \right| \binom{k+n_3}{n_3}. \quad (27)$$

Evaluating the norm of the product $\mathcal{Q}_{n_1}^{k, m_1} \mathcal{Q}_{n_2}^{k, m_2}$ and applying Hölder's inequality we obtain:

$$\begin{aligned} \|\mathcal{Q}_{n_1}^{k, m_1} \mathcal{Q}_{n_2}^{k, m_2}\|_{\tilde{V}^k} &= \sum_{n_3=0}^{n'} \left| c_{(m_1, n_1), (m_2, n_2)}^{(m_3, n_3)} \right| w_{m_3, n_3} \binom{k+n_3}{n_3} \\ &\leq \left(\sup_{0 \leq n_3 \leq n'} w_{m_3, n_3} \right) \left(\sum_{n_3=0}^{n'} \left| c_{(m_1, n_1), (m_2, n_2)}^{(m_3, n_3)} \right| \binom{k+n_3}{n_3} \right) \\ &= w_{m_3, n'} \binom{k+n_1}{n_1} \binom{k+n_2}{n_2}, \end{aligned}$$

where the last equality follows from (27) and the $w_{m, n} \leq w_{m, n+1}$ property of the weights. Furthermore as $m_3 = m_1 + m_2$ and the weights are submultiplicative $w_{m_1 + m_2, n'} \leq w_{m_1, n_1} w_{m_2, n_2}$, we obtain our first result:

$$\|\mathcal{Q}_{n_1}^{k, m_1} \mathcal{Q}_{n_2}^{k, m_2}\|_{\tilde{V}^k} \leq w_{m_1, n_1} w_{m_2, n_2} \binom{k+n_1}{n_1} \binom{k+n_2}{n_2} = \|\mathcal{Q}_{n_1}^{k, m_1}\|_{\tilde{V}^k} \|\mathcal{Q}_{n_2}^{k, m_2}\|_{\tilde{V}^k}.$$

To prove the general result, fix functions $u, v \in \tilde{V}^k$ with coefficients $a, b \in V^k$. We compute the norm of their product using our bound in (25).

$$\begin{aligned} \left\| \left(\sum_{m_1, n_1} a_{m_1, n_1} \mathcal{Q}_{n_1}^{k, m_1} \right) \left(\sum_{m_2, n_2} b_{m_2, n_2} \mathcal{Q}_{n_2}^{k, m_2} \right) \right\|_{\tilde{V}^k} &\leq \sum_{m_1, m_2, n_1, n_2} |a_{m_1, n_1} b_{m_2, n_2}| \|\mathcal{Q}_{n_1}^{k, m_1} \mathcal{Q}_{n_2}^{k, m_2}\|_{\tilde{V}^k} \\ &\leq \sum_{m_1, m_2, n_1, n_2} |a_{m_1, n_1}| \|\mathcal{Q}_{n_1}^{k, m_1}\|_{\tilde{V}^k} |b_{m_2, n_2}| \|\mathcal{Q}_{n_2}^{k, m_2}\|_{\tilde{V}^k} \\ &\leq \left\| \sum_{m_1, n_1} a_{m_1, n_1} \mathcal{Q}_{n_1}^{k, m_1} \right\|_{\tilde{V}^k} \left\| \sum_{m_2, n_2} b_{m_2, n_2} \mathcal{Q}_{n_2}^{k, m_2} \right\|_{\tilde{V}^k}. \end{aligned}$$

We have thus shown that \tilde{V}^k is a Banach algebra. As V^k and \tilde{V}^k are isometrically isomorphic, then V^k is also a Banach algebra. \square

4.3 The MMT operator for Zernike polynomials and evaluating nonlinearities

In this section we wish to provide a general framework for the product of Zernike series using the MMT approach, which is essentially the example of evaluating polynomial nonlinearity \mathcal{G} defined in (2). Since the Zernike polynomials are defined through the orthogonal Jacobi polynomials, we can make use of the theory from the previous sections. There are a couple difficulties. First, each sequence of Zernike polynomials $\{Q_n^{k,m}\}_{n \in \mathbb{N}_0}$ uses a different set of interpolation points for each pair (k, m) . Second, the function space spanned by the first N polynomials $\{Q_n^{k,m}\}_{n=0}^N$ will have polynomials of degree $2N + m$, hence the off the shelf theorems from before cannot be applied. The first issue is not a big problem if we are dealing with axisymmetric problems, a common simplifying assumption for PDEs. The second problem is easily dealt with using a change of variables.

Consider finite sequences $a \in V^{k,m_1}$ and $b \in V^{k,m_2}$ such that $a_{m_1, n_1} = 0$ and $b_{m_2, n_2} = 0$ for all $n_1 > N_1$ and $n_2 > N_2$. Suppose we are interested in computing the discrete convolution $c = a * b \in V^{k,m_3}$ for $m_3 = m_1 + m_2$, corresponding to the product:

$$\sum_{0 \leq n_3 \leq N'} c_{n_3} Q_{n_3}^{k,m_3}(r) = \left(\sum_{0 \leq n_1 \leq N_1} a_{n_1} Q_{n_1}^{k,m_1}(r) \right) \left(\sum_{0 \leq n_2 \leq N_2} b_{n_2} Q_{n_2}^{k,m_2}(r) \right),$$

where $N' = N_1 + N_2 + \frac{|m_1| + |m_2| - |m_1 + m_2|}{2}$. Recall our definition of $Q_n^{k,m}(r) = r^{|m|} P_n^{k,|m|}(x)$, where $x = 2r^2 - 1$ for $x \in [-1, 1]$. Grouping the leading powers of r , we obtain:

$$\sum_{0 \leq n_3 \leq N'} c_{n_3} P_{n_3}^{k,|m_3|}(x) = r^{|m_1| + |m_2| - |m_1 + m_2|} \left(\sum_{0 \leq n_1 \leq N_1} a_{n_1} P_{n_1}^{k,|m_1|}(x) \right) \left(\sum_{0 \leq n_2 \leq N_2} b_{n_2} P_{n_2}^{k,|m_2|}(x) \right).$$

Note that $|m_1| + |m_2| - |m_1 + m_2|$ is 0 if m_1 and m_2 are of the same sign, otherwise it is an even integer. More precisely:

$$\bar{m} \stackrel{\text{def}}{=} \frac{|m_1| + |m_2| - |m_1 + m_2|}{2} = \begin{cases} 0 & \text{if } m_1 m_2 \geq 0 \\ \min\{|m_1|, |m_2|\} & \text{otherwise.} \end{cases}$$

Thereby, we can write the leading power of r as a polynomial in x , thus obtaining:

$$\sum_{0 \leq n_3 \leq N'} c_{n_3} P_{n_3}^{k,|m_3|}(x) = \left(\frac{x+1}{2} \right)^{\bar{m}} \left(\sum_{0 \leq n_1 \leq N_1} a_{n_1} P_{n_1}^{k,|m_1|}(x) \right) \left(\sum_{0 \leq n_2 \leq N_2} b_{n_2} P_{n_2}^{k,|m_2|}(x) \right). \quad (28)$$

At this point, we are able to apply the standard interpolation methods to compute the coefficients (c_{n_3}) using the MMT and iMMT introduced in Section 2. The paradigm for computing the coefficients c_{n_3} , as summarized in Figure 1, is to evaluate the series of a and b converting them into grid-space, perform the multiplication on grid-space, and then convert back to coefficient-space.

As we are interested in multiplying series of Jacobi polynomials of potentiality different weights, on the nodes associated with Jacobi polynomials of potentiality different weights, we may need to use multiple MMT matrices, see Definition 1.1. Let us fix notation below:

Definition 4.8. For a fixed $N' \in \mathbb{N}_0$, define $M_{(k',m')}^{(k,m)}$ to be the MMT matrix evaluating the Jacobi polynomials $\{P_n^{k,m}\}_{n=0}^{N'}$ on the nodes $\{x'_i\}_{i=0}^{N'}$, given by the zeros of the Jacobi polynomial $P_{N'+1}^{k',m'}$.

Note that if $(k, m) = (k', m')$, then the entries of the iMMT matrix $[M_{(k', m')}^{(k, m)}]^{-1}$ are given by (12) given from Theorem 2.2.

The product in (28) is guaranteed to be a polynomial of degree N' , so we may exactly compute its coefficients with quadrature on N' points. Then we define the grid-space vectors $\vec{f}_0, \vec{f}_1, \vec{f}_2 \in \mathbb{R}^{N'+1}$ as:

$$(\vec{f}_0)_i = \left(\frac{x_i + 1}{2}\right)^{\bar{m}}, \quad (\vec{f}_1)_i = \sum_{0 \leq n_1 \leq N_1} a_{n_1} P_{n_1}^{k, |m_1|}(x_i), \quad (\vec{f}_2)_i = \sum_{0 \leq n_2 \leq N_2} b_{n_2} P_{n_2}^{k, |m_2|}(x_i).$$

For \vec{f}_1 and \vec{f}_2 , this may also be expressed as a matrix-vector product with the MMT matrix:

$$\vec{f}_1 = M_{(k, m_3)}^{(k, m_1)} \iota^{N'} \vec{a}, \quad \vec{f}_2 = M_{(k, m_3)}^{(k, m_2)} \iota^{N'} \vec{b},$$

for the zero section $\iota^{N'} : \mathbb{R}^{N+1} \rightarrow \mathbb{R}^{N+1} \times \mathbb{R}^{N'-N}$. Inherited from the multiplications of functions, we may define a componentwise multiplication product (also called a Hadamard product) $\odot : \mathbb{R}^{N'} \times \mathbb{R}^{N'} \rightarrow \mathbb{R}^{N'}$ for vectors $x, y \in \mathbb{R}^{N'}$ in grid space by

$$(x_1, \dots, x_{N'}) \odot (y_1, \dots, y_{N'}) \stackrel{\text{def}}{=} (x_1 y_1, \dots, x_{N'} y_{N'})$$

We may compute the output coefficients as

$$\vec{c} = [M_{(k, m_3)}^{(k, m_3)}]^{-1} \left(\vec{f}_0 \odot \vec{f}_1 \odot \vec{f}_2 \right)$$

Overall, we are able to exactly compute the coefficients in (28). While there may be rounding error from floating point arithmetic, the effects of this may be bounded using interval arithmetic.

Remark 4.9. *If $m_1 m_2 \geq 0$ and $f = f_1 = f_2$, then we get that $f_0(x) f_1(x) f_2(x) = (f(x))^2$. This corresponds exactly to the case in Section 1 with $\mathcal{G}(u) = u^2$. Furthermore, when considering more general (non-polynomial) nonlinearities, aliasing for the Zernike coefficients must be addressed. In particular, handling fractional powers of $r^{|m|}$ for the radial component is not straightforward. We leave this issue for future work.*

We also note that this method of multiplication can be modified to handle functions with different k , which is necessary in settings such as the axisymmetric Navier–Stokes equations. In such cases, different values of k are required. Nevertheless, the method works well if k_1, k_2, k_3 satisfy $k_3 = \max\{k_1, k_2\}$.

Finally, it is also worth mentioning that an alternative method of computing products (28) may be performed by first converting all of the coefficients to the same set of basis functions, and then computing the product with the MMT. More precisely, suppose now that a is a sequence in the $(P_n^{k, m_1})_{n \in \mathbb{N}}$ basis, b in the $(P_n^{k, m_2})_{n \in \mathbb{N}}$ basis and c is the $(P_n^{k, m_3})_{n \in \mathbb{N}}$ basis where $m_3 = m_1 + m_2$. Under the assumption that $m_1, m_2 \geq 0$, we convert both sequences a and b into the basis $(P_n^{k, m_3})_{n \in \mathbb{N}}$. This can be achieved through the application of a banded matrix, constructed using to the following relation (see Chapter 18.9 in [OLBC10])

$$(2n + k + m + 1) P_n^{k, m} = (n + k + m + 1) P_n^{k, m+1} + (n + k) P_{n-1}^{k, m+1}.$$

Then, one can evaluate the functions associated to a and b on the $(P_n^{k, m_3})_{n \in \mathbb{N}}$ grid points using the MMT, $M_{(k, m_3)}^{(k, m_3)}$. After performing a pointwise product, the result on the grid is transformed back to coefficients using the iMMT, $[M_{(k, m_3)}^{(k, m_3)}]^{-1}$, computed using the formula from Theorem 2.2. Indeed, this multiplication method is the one applied in our PDE applications discussed in Section 5.

4.4 Pseudo-differential Operators

Before proceeding, we take a moment to clarify the motivation for introducing pseudo-differential operators in this section. These operators are essential for extending the current framework to more complex problems, such as the axisymmetric Navier–Stokes equations or other PDEs on nontrivial geometries. By establishing their properties and interconnections here, we provide a foundation for future research that will build upon the methods and ideas presented. While some of these operators may seem peripheral to the immediate results of this work, they are critical for appreciating the broader applicability and potential of the techniques discussed. This preparatory step ensures a solid theoretical foundation for applications requiring more advanced analysis.

A central feature of the Zernike polynomials contributing to their effectiveness is that the natural differential operators on the disk yield sparse operators in coefficient space which are easy to invert [BVO⁺20, VBL⁺16]. The caveat here is that the nice representation of differential operators is only possible if we are willing to change function bases. This again is no different than the case with Chebyshev. Below we review common linear operators on the spaces of Zernike polynomials from [VBL⁺16], having appropriately modified the formulas to account for the difference in our normalization of basis elements. In particular, we derive such formulas considering $m \geq 0$, since the cases $m < 0$ can be derived using (23).

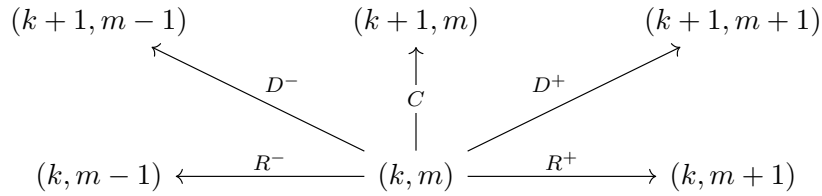


Figure 5: Various ladder operators on Zernike polynomials, figure emulated from [VBL⁺16].

On the two-dimensional disk, there are several common coordinate systems, such as Cartesian (x, y) , polar-radial (r, θ) , or complex (z, \bar{z}) . The Laplacian on the disk may be expressed in any of these coordinate systems:

$$\Delta = \partial_x^2 + \partial_y^2 = \partial_r^2 + \frac{1}{r}\partial_r + \frac{1}{r^2}\partial_\theta^2 = 4\partial_z\partial_{\bar{z}}$$

For manipulating the Zernike polynomials, the differential operators ∂_z and $\partial_{\bar{z}}$ have the most natural expression. For a motivating example, note that for a complex function $F(r, \theta) = e^{im\theta} f(r)$ with the single azimuthal wave number m , then one may compute its ∂_z and $\partial_{\bar{z}}$ derivatives, given by

$$\begin{aligned}\partial_z F(r, \theta) &= \frac{1}{2}e^{i(m-1)\theta} \left(\partial_r + \frac{m}{r} \right) f(r) \\ \partial_{\bar{z}} F(r, \theta) &= \frac{1}{2}e^{i(m+1)\theta} \left(\partial_r - \frac{m}{r} \right) f(r).\end{aligned}$$

Notice in particular that the azimuthal wave number is decreased by ∂_z , and increased by $\partial_{\bar{z}}$. Thus motivated, we define the differential operators

$$D^- \stackrel{\text{def}}{=} 2\partial_z, \quad D^+ \stackrel{\text{def}}{=} 2\partial_{\bar{z}}.$$

One may see that these operators commute, and moreover the Laplacian is given by $\Delta = D^+ D^- = D^- D^+$. The action of these operators on the Zernike polynomials is in fact easily expressed: each basis element is sent to a scalar multiple of another basis element. Specifically, given (k, m) , we

define $D_{k,m}^+ : V^{k,m} \rightarrow V^{k+1,m+1}$ (respectively $D_{k,m}^- : V^{k,m} \rightarrow V^{k+1,m-1}$) as the restriction of D^+ to $V^{k,m} \rightarrow V^{k+1,m+1}$ (respectively of D^- to $V^{k,m} \rightarrow V^{k+1,m-1}$) and obtain the following formulas (see [VBL⁺16]):

$$\begin{aligned} D_{k,m}^+ \mathcal{Q}_n^{k,m} &= 2(n+k+m+1) \mathcal{Q}_{n-1}^{k+1,m+1} && \text{if } m \geq 0, \\ D_{k,m}^- \mathcal{Q}_n^{k,m} &= 2(n+m) \mathcal{Q}_n^{k+1,m-1} && \text{if } m > 0, \end{aligned}$$

with the convention that $\mathcal{Q}_{-1}^{k,m} = 0$. The formulae for $m \leq 0$ may be easily derived by taking the complex conjugate, see (23). Furthermore, we deduce the action of the Laplacian $\Delta = D^+ D^-$ on Zernike polynomials:

$$\Delta \mathcal{Q}_n^{k,m} = 4(n+m)(n+k+m+1) \mathcal{Q}_{n-1}^{k+2,m} \stackrel{\text{def}}{=} \lambda_n^{k,m} \mathcal{Q}_{n-1}^{k+2,m}. \quad (29)$$

Moreover, when combined with Dirichlet boundary condition, we obtain the following inverse for the Laplacian.

Proposition 4.10. *[See [Jan14]] Let $m \in \mathbb{N}_0$ and let Δ_0^{-1} denote the inverse Laplacian with Dirichlet boundary conditions on the disk. Then,*

$$\Delta_0^{-1} \mathcal{Q}_n^{0,m} = \begin{cases} \frac{\mathcal{Q}_1^{0,m}}{4(m+1)(m+2)} - \frac{\mathcal{Q}_0^{0,m}}{4(m+1)(m+2)} & \text{if } n = 0 \\ \frac{\mathcal{Q}_{n+1}^{0,m}}{4(2n+m+1)(2n+m+2)} - \frac{\mathcal{Q}_n^{0,m}}{2(2n+m+2)(2n+m)} + \frac{\mathcal{Q}_{n-1}^{0,m}}{4(2n+m)(2n+m+1)} & \text{if } n \geq 1 \end{cases} \quad (30)$$

As underlined by (29), the expression of derivatives has a simple expression if we allow ourselves to change basis functions from V^k to V^{k+p} , where p is the degree of differentiation. However, when considering a zero-finding problem combining linear differential operators and nonlinearities (cf. Section 5), one often need to change basis in order for the image of the zero-finding problem to be expressed in the same basis. For this, one may define a conversion operator $C : V^k \rightarrow V^{k+1}$ which converts the V^k -coefficients of a function into the V^{k+1} -coefficients. In particular, the restriction $C_{k,m} : V^{k,m} \rightarrow V^{k+1,m}$ of C to the subspace $V^{k,m}$ is given as follows (see [VBL⁺16])

$$C_{k,m} \mathcal{Q}_n^{k,m} = \frac{n+k+m+1}{2n+k+m+1} \mathcal{Q}_n^{k+1,m} - \frac{n+m}{2n+k+m+1} \mathcal{Q}_{n-1}^{k+1,m}.$$

For instance, the operator $\Delta - I : V^{k,m} \rightarrow V^{k+2,m}$ restricted to $V^{k,m}$ writes $D_{k+1,m-1}^+ D_{k,m}^- - C_{k+1,m} C_{k,m}$ and can be expressed explicitly using the formulas given above.

Following our objective to treat PDEs on the disk, we now introduce the multiplication operators by z and by \bar{z} , which appear naturally in polar coordinates. Specifically, we define the operators R^+ and R^- as such multiplication operators :

$$R^+ f(z, \bar{z}) \stackrel{\text{def}}{=} z f(z, \bar{z}), \quad R^- f(z, \bar{z}) \stackrel{\text{def}}{=} \bar{z} f(z, \bar{z}). \quad (31)$$

The above operators have an explicit representation when expressed in the Zernike basis. Indeed, given (k, m) , we define $R_{k,m}^+ : V^{k,m} \rightarrow V^{k,m+1}$ (respectively $R_{k,m}^- : V^{k,m} \rightarrow V^{k,m-1}$) as the restriction of R^+ to $V^{k,m} \rightarrow V^{k,m+1}$ (respectively of R^- to $V^{k,m} \rightarrow V^{k,m-1}$) and obtain the following formulas (see [VBL⁺16]):

$$\begin{aligned} R_{k,m}^+ \mathcal{Q}_n^{k,m} &= \frac{n+k+|m|+1}{2n+k+|m|+1} \mathcal{Q}_n^{k,m+1} + \frac{n+k}{2n+k+|m|+1} \mathcal{Q}_{n-1}^{k,m+1}, && \text{if } m \geq 0. \\ R_{k,m}^- \mathcal{Q}_n^{k,m} &= \frac{n+1}{2n+k+|m|+1} \mathcal{Q}_{n+1}^{k,m-1} + \frac{n+|m|}{2n+k+|m|+1} \mathcal{Q}_n^{k,m-1}, && \text{if } m > 0. \end{aligned} \quad (32)$$

Again, the formulae for $m \leq 0$ may be derived by taking the complex conjugate, see (23). We summarize how the operators D^\pm , R^\pm , C all operate between the spaces $V^{k,m}$ in Figure 5. Having recalled explicit formulas for the different linear operators appearing in the study of PDEs on the disk, we are in a position to investigate specific PDE applications.

5 Applications to elliptic semilinear PDEs on the disk

The framework established in Sections 2, 3 and 4 allows the study of elliptic semilinear PDEs on the disk. In this section, we leverage these results to produce computer-assisted proofs of the existence of solutions to (4) and (5).

Using the notation established in Section 4.4 we may write the PDEs in (4) and (5) for a complex function $v : \mathbb{D} \rightarrow \mathbb{C}$ as

$$\begin{cases} \Delta v + (R^+)^{-1}v^2 = 0, & (\text{Case } m = -1) \\ \Delta v + (R^-)^m v^2 = 0, & (\text{Case } m \in \mathbb{N}_0) \end{cases} \quad (33)$$

both subject to the Dirichlet boundary conditions $v|_{\partial\mathbb{D}} = 0$. Recall from their definition in (31) that R^+ and R^- correspond to multiplications by z and \bar{z} respectively.

In general, the solutions of these PDEs may be written as series in Zernike polynomials

$$v(r, \theta) = \sum v_{m,n} \mathcal{Q}_n^{k,m}(r, \theta) = \sum v_{m,n} e^{im\theta} Q_n^{k,m}(r).$$

The PDEs do not exactly possess gauge symmetry (i.e. $f(e^{i\theta}v) = e^{i\theta}f(v)$, for all θ and $v \in \mathbb{C}$). However, for the m^{th} PDE in the family we are able to make a ‘‘generalized axisymmetric’’ assumption $v(r, \theta) = e^{im\theta}u(r)$, where $u : [0, 1] \rightarrow \mathbb{R}$. Using this ansatz, the equation reduces to an ODE in r :

$$\left(\partial_r^2 + \frac{1}{r} \partial_r - \frac{m^2}{r^2} \right) u(r) + r^m u(r)^2 = 0 \quad r \in [0, 1] \quad (34)$$

paired with the boundary condition $u(1) = 1$. Similarly, the ansatz $v(z) = e^{i\theta}u(r)$ allows to transform (5) into

$$\left(\partial_r^2 + \frac{1}{r} \partial_r - \frac{1}{r^2} \right) u(r) + \frac{1}{r} u(r)^2 = 0 \quad r \in [0, 1] \quad (35)$$

paired with the boundary condition $u(1) = 0$ and the pole condition $u(0) = 0$. This reduces the problem to looking for a real-valued solution u to (34) and (35) written as a singly indexed series:

$$u(r) = \sum_{n \in \mathbb{N}_0} u_n Q_n^{0,|m|}(r),$$

where $u_n = v_{|m|,n} \in \mathbb{R}$. Note that as $Q_n^{0,|m|} = r^{|m|} P_n^{0,|m|}(2r^2 - 1)$, the pole condition $u^{(k)}(0) = 0$ is satisfied for all $k < |m|$.

5.1 Formulation as a $F(x) = 0$ problem

In order to apply Theorem 3.1, we will explicitly define a functional equation $F_m : X \rightarrow X'$ whose zeros correspond to solutions of (33). Resulting from our generalized axisymmetric assumption we fix $X = X' \stackrel{\text{def}}{=} V^{0,|m|}$, as defined in (24), to be the sequence space of Zernike polynomials with fixed

wave number $|m|$. The norm on this space is inherited from V^0 given in Definition 4.4, and in this paper we will work with trivial weights (i.e. $\langle m, n \rangle = 1$ for all m, n).

While formally $V^{0,|m|} \subseteq V^0$ consists of doubly indexed sequences $U = (U_{m,n})_{m \in \mathbb{Z}, n \in \mathbb{N}_0}$ where $U_{m',n} = 0$ whenever $m' \neq m$, we may readily identify the elements with singly indexed sequences $\tilde{U} \stackrel{\text{def}}{=} (U_{m,n})_{n \in \mathbb{N}_0}$. In particular, since $k = 0$, we might think about $V^{0,|m|}$ as the usual Lebesgue space for sequences $\ell^1(\mathbb{N}_0)$. In order to keep track of the index m , we will keep the notation $V^{0,|m|}$ but use the usual notation $\|\cdot\|_1$ for the 1-norm associated to $V^{0,|m|}$. Additionally, for bounded linear operators $B(V^{0,|m|}, V^{0,|m|})$ we will similarly use the notation $\|\cdot\|_1$.

Using the notation of Section 4.4, we may encode the PDE in (33) as a functional equation in the space of Zernike coefficients. One approach to this would be to directly encode the equation; the disk Laplacian $\Delta = D^+D^-$ has a simple expression as an operator from V^k to V^{k+2} , and an additional equation could be appended to enforce the boundary condition $0 = u(1) = \sum_{n \in \mathbb{N}_0} u_n$. However it is easier to work with the inverse Dirichlet Laplacian Δ_0^{-1} , whose action on Zernike polynomials is explicitly given in Proposition 4.10.

Definition 5.1. Fix the quadratic nonlinearity $G : V^0 \rightarrow V^0$ as $G(U) = U * U$ and the inverse Laplacian Δ_0^{-1} as in Proposition 4.10. We define the family of functions $F_m : V^{0,|m|} \rightarrow V^{0,|m|}$ for each $m \in \mathbb{N}_0 \cup \{-1\}$ as

$$F_m(U) \stackrel{\text{def}}{=} \begin{cases} U + \Delta_0^{-1} \left((R_{0,1}^+)^{-1} G(U) \right) & \text{if } m = -1 \\ U + \Delta_0^{-1} \left((R^-)^m G(U) \right) & \text{if } m \in \mathbb{N}_0. \end{cases} \quad (36)$$

where $R_{0,1}^+$ is the restriction of R^+ to $V^{0,1} \rightarrow V^{0,2}$.

Finally, we introduce the spaces $V_s^{k,m}$, which are special cases of the ones introduced in Section 4.2 with algebraic weights. Such spaces are natural for the definition of differential operators. Specifically, the index s allows to keep track of the degree of differentiability associated to the series representation of the sequence.

Definition 5.2. Define $V_s^{k,m}$ as the special case of the spaces $V^{k,m}$ in (24) for which $\omega_{m,n} = (1 + 2n + |m|)^s$.

In the following lemma, we show that the maps F_m are well defined, and their zeros correspond to solutions of the PDE in (33). In particular, the spaces $V_s^{k,m}$ allow us to use a bootstrapping argument, leading to the regularity of solutions.

Lemma 5.3. Fix $m \in \mathbb{N}_0 \cup \{-1\}$. The function $F_m : V^{0,|m|} \rightarrow V^{0,|m|}$ is well defined and Fréchet differentiable. Furthermore if $\tilde{U} \in V^{0,|m|}$ is a zero of F_m , then its corresponding function $\tilde{u} = \mathcal{M}[\tilde{U}]$ is infinitely differentiable and solves the PDE (33).

Proof. To show the function is well defined, note first from Proposition 4.6 that G restricts to a map from $V^{0,|m|}$ to $V^{0,2|m|}$. Furthermore the operators R^\pm restrict to maps from $V^{0,m'}$ to $V^{0,m' \pm 1}$ for all $m' \geq 0$. It follows that F_m is well defined as a map from $V^{0,|m|}$ to $V^{0,|m|}$, at least for $m \geq 0$.

In the case of $m = -1$, there is an added complication of the operator $(R_{0,1}^+)^{-1}$, which is unbounded and only densely defined. Nevertheless, we show in Lemma A.1 that $R_{0,1}^+ : V^{0,1} \rightarrow V^{0,2}$ has a bounded inverse as a map between differently weighted spaces, in particular that $(R_{0,1}^+)^{-1} : V_s^{0,2} \rightarrow V_{s-1}^{0,1}$ is a bounded linear operator for all $s \geq 0$.

From Proposition 4.10 we have that $\Delta_0^{-1} : V_s^{k,|m|} \rightarrow V_{s+2}^{k,|m|}$ is a bounded linear operator, and from Lemma 4.7 we have that $G : V_s^{k,|m|} \rightarrow V_s^{k,2|m|}$ is smooth with Fréchet derivative $DG(x)h =$

$2x * h$ for all $x, h \in V_s^{k,|m|}$. It then follows that the compositions $\Delta_0^{-1}(R_{0,1}^+)^{-1}G(U) : V_s^{k,|m|} \rightarrow V_{s+1}^{k,|m|}$ and $\Delta_0^{-1}(R^-)^m G(U) : V_s^{k,|m|} \rightarrow V_{s+2}^{k,|m|}$ are well defined and Frechét differentiable, as are all functions $F_m : V^{0,|m|} \rightarrow V^{0,|m|}$.

The solutions being infinitely smooth follows from a standard bootstrapping argument: make the inductive assumption that $\tilde{U} \in V_s^{0,|m|}$. If $F(\tilde{U}) = 0$, then $\tilde{U} = -\Delta_0^{-1}(R_{0,1}^+)^{-1}G(\tilde{U})$ in the case $m = -1$, and $\tilde{U} = -\Delta_0^{-1}(R^-)^m G(\tilde{U})$ in the case $m \geq 0$. By the preceding argument we demonstrated that the right hand side of these equations is smoothing, hence $\tilde{U} \in V_{s+1}^{0,|m|}$ in the case $m = -1$, and $\tilde{U} \in V_{s+2}^{0,|m|}$ in the case $m \geq 0$. Since $\tilde{U} \in V_0^{0,|m|}$ by the hypothesis of this lemma, it follows by induction that $\tilde{U} \in V_s^{0,|m|}$ for all $s \geq 0$.

Furthermore, note that any derivatives of $\tilde{u} = \mathcal{M}(\tilde{U})$ may be obtained as a combination of $D^- = 2\partial_z$ and $D^+ = 2\partial_{\bar{z}}$. Since $\tilde{U} \in V_s^{0,|m|}$ for all $s \geq 0$, and the ladder operators $D_{k,m}^\pm : V_s^k \rightarrow V_{s-2}^{k+1}$ are bounded, it follows that the derivatives of \tilde{u} will have bounded Zernike coefficients in V_s^k for all $s \geq 0$. Hence $\tilde{u} \in C^\infty(\mathbb{D}, \mathbb{C})$. As \tilde{u} is smooth it satisfies (33) in the strong sense. Lastly, as $\tilde{U} = -\Delta_0^{-1}(R_{0,1}^+)^{-1}G(\tilde{U})$ in the case $m = -1$ (respectively $\tilde{U} = -\Delta_0^{-1}(R^-)^m G(\tilde{U})$ in the case $m \geq 0$), we see that \tilde{U} is in the image of the inverse Dirichlet Laplacian, and thereby satisfies Dirichlet-0 boundary conditions. \square

5.2 Computer-assisted analysis

Lemma 5.3 shows that zeros of F_m in $V^{0,|m|}$ provide smooth solutions to (4) and (5). We are now in a position to present our computer-assisted approach to prove the existence of solutions to (36). Our goal is to use Theorem 3.1 in order to prove the existence of a zero of F_m given in (36). In particular, we assume that we have access to some $U_0 \in V^{0,|m|}$, which is an approximate zero of F_m and $A : V^{0,|m|} \rightarrow V^{0,|m|}$, which is a bounded linear operator approximating the inverse of $DF_m(U_0)$. In practice, both U_0 and A will be constructed numerically.

Indeed, let us fix $N \in \mathbb{N}$ representing the size of the numerical truncation and define the following projection operators

$$\pi^N(V) = \begin{cases} v_n, & n \in I^N \\ 0, & n \notin I^N \end{cases} \quad \text{and} \quad \pi^\infty(V) = \begin{cases} 0, & n \in I^N \\ v_n, & n \notin I^N \end{cases}$$

where $I^N \stackrel{\text{def}}{=} \{n \in \mathbb{N}_0, n \leq N\}$ for all $V = (v_n)_{n \in \mathbb{N}_0} \in V^{0,|m|}$. In particular, numerically we build U_0 such that $U_0 = \pi^N U_0$, meaning that U_0 only has a finite number of non-zero coefficients (U_0 can be seen as a vector) which is stored on the computer. Its construction is obtained using a Newton method (see [Cad24] for additional details).

5.2.1 Construction of the approximate inverse A

Now that the approximate solution U_0 is fixed, we present the construction of an approximate inverse A for $DF_m(U_0)$. First, noticing that $DF_m(U_0)$ is a compact perturbation of the identity, we look for A as a finite-rank perturbation of the identity as well. In other words, we numerically construct A^N satisfying $A^N = \pi^N A^N \pi^N$ (A^N can be seen as a $N + 1$ by $N + 1$ matrix) and such that A^N approximates the inverse of the Galerkin projection of $DF_m(U_0)$ of size N , namely $\pi^N DF_m(U_0) \pi^N$. Then we define $A : V^{0,|m|} \rightarrow V^{0,|m|}$ as

$$A \stackrel{\text{def}}{=} A^N + \pi^\infty.$$

Intuitively, the tail of the operator A acts as the identity. We will show in Lemma 5.5 that this construction is justified when N is big enough.

Now that U_0 and A are constructed, following Theorem 3.1, it remains to compute the bounds Y_0, Z_1 and Z_2 introduced in the theorem.

5.2.2 Computation of the bounds

Lemma 5.4. *Let Y_0 satisfying*

$$Y_0 \geq \begin{cases} \|A^N(U_0 + \pi^N \Delta_0^{-1}(R^-)^m(U_0 * U_0))\|_1 + \|(\pi^{2N+m+1} - \pi^N)\Delta_0^{-1}(R^-)^m(U_0 * U_0)\|_1 & \text{if } m \in \mathbb{N}_0 \\ \|A^N(U_0 + \pi^N \Delta_0^{-1}(R_{0,1}^+)^{-1}(U_0 * U_0))\|_1 + \|(\pi^{2N+1} - \pi^N)\Delta_0^{-1}(R_{0,1}^+)^{-1}(U_0 * U_0)\|_1 & \text{if } m = -1 \end{cases}$$

then $\|AF_m(U_0)\|_1 \leq Y_0$.

Proof. Suppose that $m \in \mathbb{N}_0$. Then, notice that since $U_0 = \pi^N U_0$, then U_0 represents a polynomial of order $2N + m$ and consequently, $U_0 * U_0$ represents a polynomial of order $4N + 2m$. This implies that $U_0 * U_0 = \pi^{2N} U_0 * U_0$, when $U_0 * U_0$ is written in $V^{0,2m}$. Then, as $(R^-)^m$ is lower triangular and banded, with a band of size m , we obtain $(R^-)^m(U_0 * U_0) = \pi^{2N+m}(R^-)^m(U_0 * U_0)$. Finally, using (30), we have $\Delta_0^{-1}(R^-)^m(U_0 * U_0) = \pi^{2N+m+1}\Delta_0^{-1}(R^-)^m(U_0 * U_0)$. Therefore, we have

$$\begin{aligned} \|AF_m(U_0)\|_1 &= \|A^N(U_0 + \Delta_0^{-1}(R^-)^m(U_0 * U_0))\|_1 + \|\pi^\infty \Delta_0^{-1}(R^-)^m(U_0 * U_0)\|_1 \\ &= \|A^N(U_0 + \pi^N \Delta_0^{-1}(R^-)^m(U_0 * U_0))\|_1 + \|(\pi^{2N+m+1} - \pi^N)\Delta_0^{-1}(R^-)^m(U_0 * U_0)\|_1. \end{aligned}$$

Suppose now that $m = -1$. Then, as $(R_{0,1}^+)^{-1}$ is upper triangular (cf. (39)), we obtain that $(R_{0,1}^+)^{-1}(U_0 * U_0) = \pi^{2N}(R_{0,1}^+)^{-1}(U_0 * U_0)$. Moreover, using (30), we have $\Delta_0^{-1}(R_{0,1}^+)^{-1}(U_0 * U_0) = \pi^{2N+1}\Delta_0^{-1}(R_{0,1}^+)^{-1}(U_0 * U_0)$. We conclude the proof in a similar fashion as the case $m \in \mathbb{N}_0$. \square

Lemma 5.5. *Let $Z_{0,m}$ be a bound satisfying*

$$Z_{0,m} \geq \begin{cases} \|\pi^N - A^N(I + \Delta_0^{-1}(R^-)^m DG(U_0)\pi^N)\|_1 & \text{if } m \in \mathbb{N}_0 \\ \|\pi^N - A^N(I + \Delta_0^{-1}(R_{0,1}^+)^{-1} DG(U_0))\pi^N\|_1 & \text{if } m = -1. \end{cases}$$

If Z_1 satisfies

$$Z_1 \geq \begin{cases} \max\{Z_{0,m}, \|A^N \Delta_0^{-1}(R^-)^m DG(U_0)(\pi^{2N+m+1} - \pi^N)\|_1\} + \frac{2\|U_0\|_1}{(2(N+1)+m)^2} & \text{if } m \in \mathbb{N}_0 \\ \max\{Z_{0,-1}, \|A^N \Delta_0^{-1} DG((R_{0,0}^+)^{-1} U_0)(\pi^{2N+1} - \pi^N)\|_1\} + \frac{\|(R_{0,0}^+)^{-1} U_0\|_1}{2N^2} & \text{if } m = -1 \end{cases}$$

then $\|I - ADF_m(U_0)\|_1 \leq Z_1$.

Proof. Suppose that $m \in \mathbb{N}_0$. Then,

$$\begin{aligned} \|I - ADF_m(U_0)\|_1 &= \|\pi^N + \pi^\infty - (A^N + \pi^\infty)(I + \Delta_0^{-1}(R^-)^m DG(U_0))\|_1 \\ &\leq \|\pi^N - A^N(I + \Delta_0^{-1}(R^-)^m DG(U_0))\|_1 + \|\pi^\infty \Delta_0^{-1}(R^-)^m DG(U_0)\|_1. \end{aligned}$$

Now, notice that because $U_0 = \pi^N U_0$, then

$$\pi^N \Delta_0^{-1}(R^-)^m DG(U_0) = \pi^N \Delta_0^{-1}(R^-)^m DG(U_0)\pi^{2N+m+1},$$

using the same reasoning as for the proof of Lemma 5.4. Moreover, we have

$$\begin{aligned} & \|\pi^N - A^N \Delta_0^{-1} (R^-)^m DG(U_0) \pi^{2N+m+1}\|_1 \\ & \leq \max \left\{ \|\pi^N - A^N \Delta_0^{-1} (R^-)^m DG(U_0) \pi^N\|_1, \|A^N \Delta_0^{-1} (R^-)^m DG(U_0) (\pi^{2N+m+1} - \pi^N)\|_1 \right\}. \end{aligned}$$

Finally, notice from (30) that we have the operator bound:

$$\begin{aligned} \|\pi^\infty \Delta_0^{-1}\|_1 &= \sup_{n \geq N+1} \left\| \frac{\pi_\infty \mathcal{Q}_{n+1}^{0,m}}{4(2n+m+1)(2n+m+2)} - \frac{\pi_\infty \mathcal{Q}_n^{0,m}}{2(2n+m+2)(2n+m)} + \frac{\pi_\infty \mathcal{Q}_{n-1}^{0,m}}{4(2n+m)(2n+m+1)} \right\|_1 \\ &\leq \frac{1}{(2(N+1)+m)^2}, \end{aligned}$$

and thereby we obtain:

$$\|\pi^\infty \Delta_0^{-1} (R^-)^m DG(U_0)\|_1 \leq \|\pi^\infty \Delta_0^{-1}\|_1 \|(R^-)^m DG(U_0)\|_1 \leq \frac{1}{(2(N+1)+m)^2} \|(R^-)^m\|_1 \|2U_0\|_1.$$

We conclude the proof of the case $m \in \mathbb{N}_0$ using (38).

Suppose now that $m = -1$. We have

$$\begin{aligned} \|I - ADF_m(U_0)\|_1 &= \|\pi^N + \pi^\infty - (A^N + \pi^\infty)(I + \Delta_0^{-1} (R_{0,1}^+)^{-1} DG(U_0))\|_1 \\ &\leq \|\pi^N - A^N (I + \Delta_0^{-1} (R_{0,1}^+)^{-1} DG(U_0)) + \pi^\infty \Delta_0^{-1} (R_{0,1}^+)^{-1} DG(U_0)\|_1 \\ &\leq \|\pi^N - A^N (I + \Delta_0^{-1} (R_{0,1}^+)^{-1} DG(U_0))\|_1 + \|\pi^\infty \Delta_0^{-1} (R_{0,1}^+)^{-1} DG(U_0)\|_1. \end{aligned}$$

Now, given $W \in V^{0,1}$, notice that

$$(R_{0,1}^+)^{-1} (U_0 * W) = \left((R_{0,0}^+)^{-1} U_0 \right) * W \quad (37)$$

since $\frac{1}{r}(u_0 w) = \frac{u_0}{r} w$ if w is the function representation of W . Consequently, we obtain the following

$$\begin{aligned} \|\pi_\infty \Delta_0^{-1} (R_{0,1}^+)^{-1} DG(U_0)\|_1 &\leq \|\pi_\infty \Delta_0^{-1}\|_1 \|(R_{0,1}^+)^{-1} DG(U_0)\|_1 = \frac{1}{4N^2} \sup_{\|h\|=1} \|(R_{0,1}^+)^{-1} (2U_0 * h)\|_1 \\ &= \frac{1}{2N^2} \|(R_{0,0}^+)^{-1} U_0\|_1. \end{aligned}$$

Then,

$$\begin{aligned} & \|\pi^N - A^N (I + \Delta_0^{-1} (R_{0,1}^+)^{-1} DG(U_0))\|_1 \\ &= \max \left\{ \|\pi^N - A^N (I + \Delta_0^{-1} (R_{0,1}^+)^{-1} DG(U_0)) \pi^N\|_1, \|A^N \Delta_0^{-1} (R_{0,1}^+)^{-1} DG(U_0) \pi^\infty\|_1 \right\}. \end{aligned}$$

Finally, using (37), we have that

$$(R_{0,1}^+)^{-1} DG(U_0) = DG \left((R_{0,0}^+)^{-1} U_0 \right)$$

since G is quadratic. Now, using (41), we have that $(R_{0,0}^+)^{-1}$ is upper triangular and therefore $(R_{0,0}^+)^{-1} U_0 = \pi^N (R_{0,0}^+)^{-1} U_0$. This yields

$$\begin{aligned} \|A^N \Delta_0^{-1} (R_{0,1}^+)^{-1} DG(U_0) \pi^\infty\|_1 &= \|A^N \Delta_0^{-1} DG \left((R_{0,0}^+)^{-1} U_0 \right) \pi^\infty\|_1 \\ &= \|A^N \Delta_0^{-1} DG \left((R_{0,0}^+)^{-1} U_0 \right) (\pi^{2N+1} - \pi^N)\|_1. \quad \square \end{aligned}$$

Lemma 5.6. *Let Z_2 be a bound satisfying*

$$Z_2 \geq \begin{cases} 2\|A^N \Delta_0^{-1}(R^-)^m \pi^{N+1}\|_1 + \frac{2}{(2(N+1)+m)^2} & \text{if } m \in \mathbb{N}_0 \\ 2\|A^N \Delta_0^{-1}(R_{0,1}^+)^{-1} \pi^N\|_1 + \frac{16}{15} \frac{\|A^N\|_1}{N+3} + \frac{1}{2N} & \text{if } m = -1 \end{cases}$$

then $\|A(DF_m(c) - DF_m(U_0))\|_1 \leq Z_2 r$ for all $c \in \overline{B_r(U_0)}$.

Proof. Along the proof, given Banach spaces X, Y , we denote $\|\cdot\|_{B(X,Y)}$ as the operator norm for bounded linear operators on $X \rightarrow Y$. Suppose that $m \in \mathbb{N}_0$. Then, given $c \in \overline{B_r(U_0)}$, we have

$$\begin{aligned} \|A(DF_m(c) - DF_m(U_0))\|_1 &= \|A \Delta_0^{-1}(R^-)^m DG(c - U_0)\|_1 \\ &\leq \|A^N \Delta_0^{-1}(R^-)^m DG(c - U_0)\|_1 + \|\pi^\infty \Delta_0^{-1}(R^-)^m DG(c - U_0)\|_1, \end{aligned}$$

where we used that $DG(c) - DG(U_0) = DG(c - U_0)$ since G is quadratic. Now, notice that

$$\|\pi^\infty \Delta_0^{-1}(R^-)^m DG(c - U_0)\|_1 \leq \frac{2}{(2(N+1)+m)^2} \|(R^-)^m\|_1 \|c - U_0\|_1 \leq \frac{1}{2N^2} \|(R^-)^m\|_1 r$$

and

$$\begin{aligned} \|A^N \Delta_0^{-1}(R^-)^m DG(c - U_0)\|_1 &= \|A^N \Delta_0^{-1} \pi^{N+1}(R^-)^m DG(c - U_0)\|_1 \\ &\leq 2\|A^N \Delta_0^{-1}(R^-)^m \pi^{N+1}\|_1 r. \end{aligned}$$

We conclude the proof of the case $m \in \mathbb{N}_0$ using (38).

For the case $m = -1$, we have

$$\begin{aligned} \|A(DF_m(c) - DF_m(U_0))\|_1 &= \|A \Delta_0^{-1}(R_{0,1}^+)^{-1} DG(c - U_0)\|_1 \\ &\leq \|A^N \Delta_0^{-1}(R_{0,1}^+)^{-1} DG(c - U_0)\|_1 + \|\pi^\infty \Delta_0^{-1}(R_{0,1}^+)^{-1} DG(c - U_0)\|_1. \end{aligned}$$

Now, combining Definition 5.2 with (30), we obtain that

$$\|\pi^\infty \Delta_0^{-1}\|_{B(V_{-1}^{0,1}, V_0^{0,1})} \leq \sup_{n \geq N+1} \frac{1}{(2n+2)^{-1}} \left(\frac{1}{4(2n+2)(2n+3)} + \frac{1}{2(2n+3)(2n+1)} + \frac{1}{4(2n+1)(2n+2)} \right) \leq \frac{1}{2N}$$

Then, using (40), we get

$$\|\pi^\infty \Delta_0^{-1}(R_{0,1}^+)^{-1} DG(c - U_0)\|_1 \leq \|\pi^\infty \Delta_0^{-1}\|_{B(V_{-1}^{0,1}, V_0^{0,1})} \|(R_{0,1}^+)^{-1}\|_{B(V_0^{0,2}, V_{-1}^{0,1})} \|DG(c - U_0)\|_1 \leq \frac{1}{2N} r.$$

Now, notice that we have

$$\begin{aligned} \|A^N \Delta_0^{-1}(R_{0,1}^+)^{-1} \pi^\infty DG(c - U_0)\|_1 &\leq \|A^N\|_1 \|\Delta_0^{-1}\|_{B(V_{-2}^{0,1}, V_0^{0,1})} \|(R_{0,1}^+)^{-1} \pi^\infty\|_{B(V_0^{0,2}, V_{-2}^{0,1})} \|DG(c - U_0)\|_1 \\ &\leq 2\|A^N\|_1 \|\Delta_0^{-1}\|_{B(V_{-2}^{0,1}, V_0^{0,1})} \|(R_{0,1}^+)^{-1} \pi^\infty\|_{B(V_0^{0,2}, V_{-2}^{0,1})} r. \end{aligned}$$

Then using (43), we get

$$\|(R_{0,1}^+)^{-1} \pi^\infty\|_{B(V_0^{0,2}, V_{-2}^{0,1})} = \max_{j > N} \left\{ \sum_{i=0}^j \frac{1}{2(j+1)(j+2)} \right\} = \frac{1}{2(N+3)}.$$

Also we have the bound

$$\|\Delta_0^{-1}\|_{B(V_{-2}^{0,1}, V_0^{0,1})} \leq \max \left\{ \frac{1}{3}, \sup_{n \geq 1} \frac{1}{(2n+2)^{-2}} \left(\frac{1}{4(2n+2)(2n+3)} + \frac{1}{2(2n+3)(2n+1)} + \frac{1}{4(2n+1)(2n+2)} \right) \right\} \leq \frac{16}{15}.$$

Consequently, using a similar reasoning as what was achieved above, we get

$$\begin{aligned} \|A^N \Delta_0^{-1}(R_{0,1}^+)^{-1} DG(c - U_0)\|_1 &\leq \|A^N \Delta_0^{-1}(R_{0,1}^+)^{-1} \pi^N DG(c - U_0)\|_1 + \|A^N \Delta_0^{-1}(R_{0,1}^+)^{-1} \pi^\infty DG(c - U_0)\|_1 \\ &\leq 2\|A^N \Delta_0^{-1}(R_{0,1}^+)^{-1} \pi^N\|_1 r + \frac{16}{15} \frac{\|A^N\|_1}{N+3} r. \end{aligned} \quad \square$$

5.3 Existence proofs for different values of m

In this section we present some computer-assisted proofs of existence of non-trivial solutions to (4) with $m = -1, 0, 1, 2, 20$. For each value of m , we denote by $U_{0,m}$, the associated approximate solution used in the proof and provide its function representation (real part) in the figures below. The approximate solution is obtained numerically using the procedure described in [Cad24]. Moreover, we provide the numerical quantities related to the proof in Table 1.

In the proofs, we use extended precision to compute and store the MMT and iMMT matrices. Specifically, we use 128 bits to represent the matrices thanks to the “BigFloat” type in Julia. This extension of the precision allows us to compute products with high accuracy. The rest of the computations are run in standard double floating point arithmetic.

Theorem 5.7. *Let $m \in \{-1, 0, 1, 2, 20\}$ and let $r_m > 0$ be its associated value as given in Table 1. Then, there exists $\tilde{U}_m \in V^{0,|m|}$, such that \tilde{U}_m solves (36) and $\tilde{U}_m \in \overline{B_{r_m}(U_{0,m})}$.*

Table 1: Verified quantities of Theorem 3.1

Value of m	Y_0	Z_1	Z_2	N	$\ U_{0,m}\ _1$	Value of r_m
-1	1.57×10^{-14}	1.49×10^{-1}	0.46	36	17	1.85×10^{-14}
0	7.62×10^{-16}	4.28×10^{-3}	0.71	36	8.6	7.65×10^{-16}
1	2.89×10^{-14}	2.36×10^{-2}	0.14	36	59	2.96×10^{-14}
2	5.34×10^{-14}	5.61×10^{-2}	0.058	36	151	5.66×10^{-14}
20	1.52×10^{-7}	8.86×10^{-1}	0.0013	75	9900	1.33×10^{-6}

Notice that for positive values of m , the maximal amplitude increases as m increases. In particular, for $m = 20$, we need to increase the number of coefficients in order to approximate accurately the solution and obtain a proof of existence. In particular, this has a detrimental effect on the quality of the radius r_{20} compared to the other solutions. Note, however, that this could be resolved by performing the whole computer-assisted proof in extended precision (whereas, for now, only products are implemented in extended precision).

Conclusion and Future Work

In this manuscript, we introduced a computer-assisted framework for the rigorous evaluate of polynomial nonlinearities at series expansions of orthogonal polynomials. Specifically, this methodology is applied to Zernike polynomials, enabling the analysis of nonlinear PDEs on the disk. Several extensions of this work are possible. For instance, one could consider tensor products of Zernike polynomials with Fourier series, which would naturally facilitate the study of PDEs on cylindrical domains with periodic boundary conditions in the vertical direction. Such spatial domains have been explored, for example, in the context of the axisymmetric Navier–Stokes equations [Hou23, HH23]. On the technical side, however, this tensor product introduces more intricate operator structures on sequences, which would require detailed analysis to enable computer-assisted proofs. This extension is currently under investigation.

Another promising direction for future work is the treatment of nonpolynomial nonlinearities. For instance, extending our methodology to PDEs with exponentials in the nonlinearity — such as the Karma system, which is used to model spiral wave breakup in cardiac tissue [Kar93, Kar94, DS19] — would require adaptations. Specifically, given a finite polynomial $u(x) = \sum_{n=0}^N a_n p_n(x)$, where $\{p_n\}$ is a family of orthogonal polynomials, the nonlinear transformation $\mathcal{G}(u)$ yields an

infinite sequence of coefficients, as opposed to the finite representation possible for polynomial nonlinearities. To address this, one would need to develop a Poisson-like formula, akin to those used in conjunction with the Fourier Discrete Transform, and employ precise techniques from complex analysis to rigorously estimate the coefficients of $\mathcal{G}(u)$.

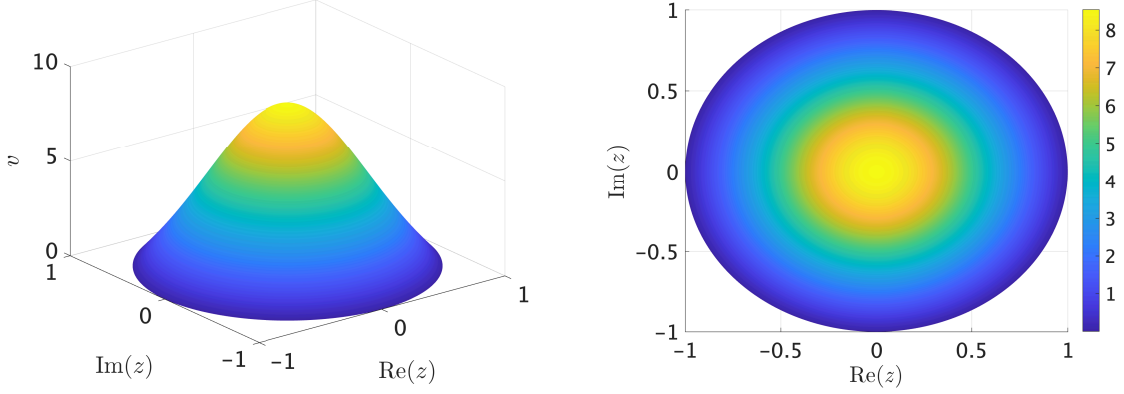


Figure 6: Real part of the approximate solution with $m = 0$.

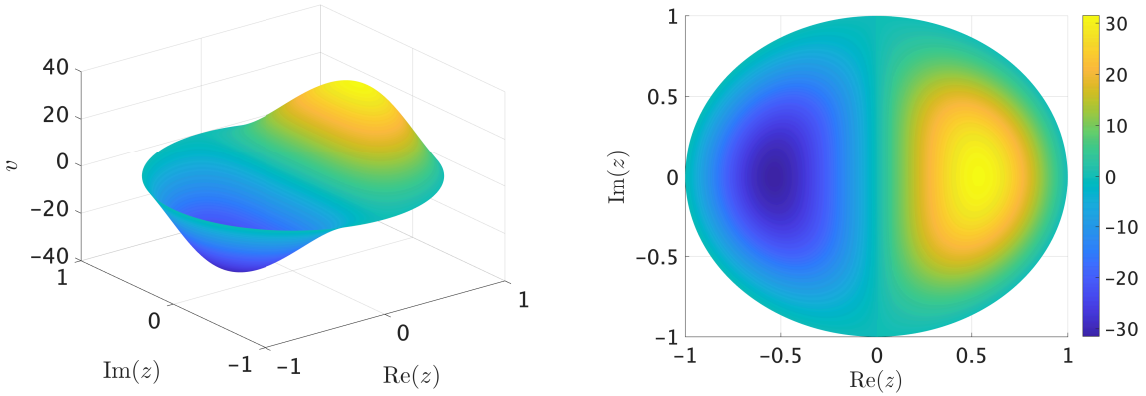


Figure 7: Real part of the approximate solution with $m = 1$.

A Some operator Bounds

Recalling the definition of the operator R^- in (32), we can define the multiplication operator by z^m on $V^{0,2m} \rightarrow V^{0,m}$, that we denote $(R^-)^m$, as follows

$$(R^-)^m: V^{0,2m} \xrightarrow{R^-} V^{0,2m-1} \xrightarrow{R^-} V^{0,2m-2} \dots \xrightarrow{R^-} V^{0,m+1} \xrightarrow{R^-} V^{0,m}$$

Using that R^- is lower triangular, we readily have

$$\|R^-\|_1 = \max_{m \in \mathbb{Z}} \max_{n \in \mathbb{N}_0} \left\{ \frac{n+1}{2n+m+1} + \frac{n+m}{2n+m+1} \right\} = 1.$$

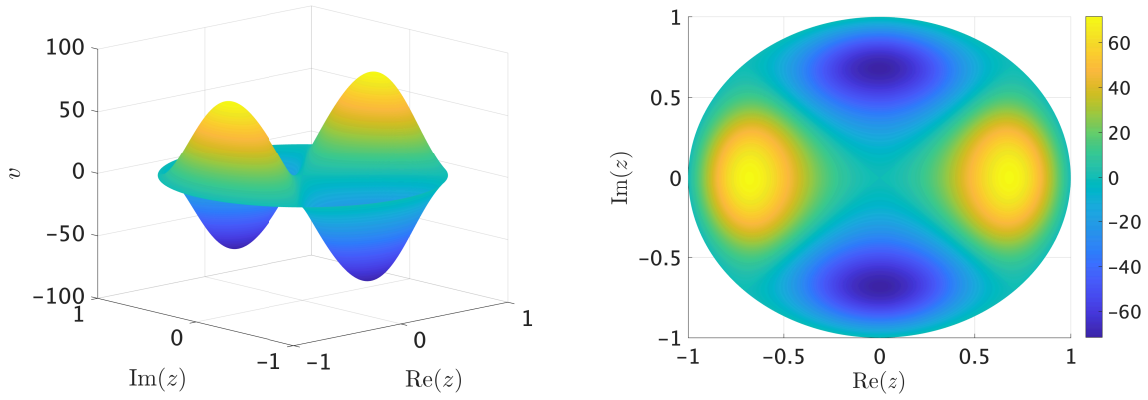


Figure 8: Real part of the approximate solution with $m = 2$.

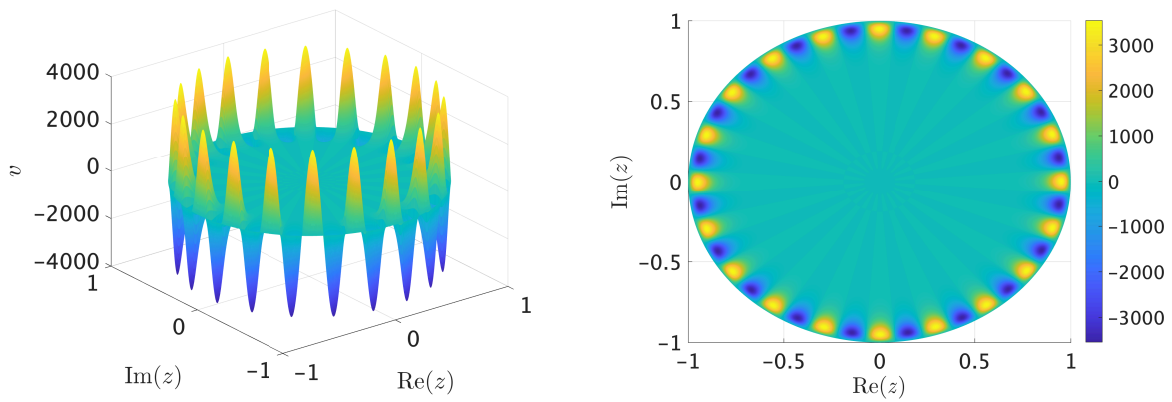


Figure 9: Real part of the approximate solution with $m = 20$.

Consequently, this implies that

$$\|(R^-)^m\|_1 \leq 1. \quad (38)$$

Now, recall that we define $R_{0,1}^+ : V^{0,1} \rightarrow V^{0,2}$ (resp. $R_{0,0}^+ : V^{0,0} \rightarrow V^{0,1}$) as the restriction of R^+ (cf. (32)) to $V^{0,1} \rightarrow V^{0,2}$ (resp. $V^{0,0} \rightarrow V^{0,1}$). Consequently, both $R_{0,0}^+$ and $R_{0,1}^+$ can be represented as upper-triangular linear operators on sequences indexed on \mathbb{N}_0 . The following lemma provides an explicit inverse for $R_{0,0}^+$ and $R_{0,1}^+$ which will be used for computing the estimates in Section 5.2.

Lemma A.1. *The operator $R_{0,1}^+ : V_s^{0,1} \rightarrow V_{s-1}^{0,2}$ is invertible and its inverse, denoted $(R_{0,1}^+)^{-1} : V_s^{0,2} \rightarrow V_{s-1}^{0,1}$, is given by*

$$\left((R_{0,1}^+)^{-1} \right)_{i,j} = \begin{cases} (-1)^{j+i} \frac{2(i+1)^2}{(j+1)(j+2)} & \text{if } j \geq i \\ 0 & \text{otherwise.} \end{cases} \quad (39)$$

Moreover,

$$\|(R_{0,1}^+)^{-1}\|_{B(V_0^{0,2}, V_{-1}^{0,1})} \leq \frac{1}{2}, \quad (40)$$

where $\|\cdot\|_{B(V_0^{0,2}, V_{-1}^{0,1})}$ denotes the operator norm for bounded linear operators on $V_0^{0,2} \rightarrow V_{-1}^{0,1}$. Similarly, $R_{0,0}^+ : V_s^{0,0} \rightarrow V_{s-1}^{0,1}$ is invertible and its inverse, denoted $(R_{0,0}^+)^{-1} : V_s^{0,1} \rightarrow V_{s-1}^{0,0}$, is given by

$$\left((R_{0,0}^+)^{-1} \right)_{i,j} = \begin{cases} (-1)^{j+i} \frac{2i+1}{j+1} & \text{if } j \geq i \\ 0 & \text{otherwise.} \end{cases} \quad (41)$$

Proof. Let $f = (f_i)_{i \in \mathbb{N}_0} \in V^{0,2}$. First recall from (32) that $R_{0,m}^+ \mathcal{Q}_i^{0,m} = \frac{i+|m|+1}{2i+|m|+1} \mathcal{Q}_i^{0,m+1} + \frac{i}{2i+|m|+1} \mathcal{Q}_{i-1}^{0,m+1}$. Suppose that we have define $\alpha_i = \frac{i+2}{2(i+1)}$ and $\beta_i = \frac{i}{2i+2}$, then, in order to invert $R_{0,1}^+$, we need to find $x = (x_i)_{i \in \mathbb{N}_0}$ satisfying

$$\alpha_i x_i + \beta_{i+1} x_{i+1} = f_i$$

for all $i \in \mathbb{N}_0$. The above is equivalent to

$$x_i = \frac{f_i}{\alpha_i} - \frac{\beta_{i+1}}{\alpha_i} x_{i+1} = \frac{f_i}{\alpha_i} - \frac{\beta_{i+1}}{\alpha_i} \left(\frac{f_{i+1}}{\alpha_{i+1}} - \frac{\beta_{i+2}}{\alpha_{i+1}} x_{i+2} \right) = \sum_{j=i}^{\infty} (-1)^{i+j} \frac{\beta_{i+1} \cdots \beta_j}{\alpha_i \cdots \alpha_j} f_j \quad (42)$$

since $f_j \rightarrow 0$ as $j \rightarrow \infty$. In particular, we have

$$\frac{\beta_j}{\alpha_j} = \frac{j}{j+2}$$

and therefore,

$$\frac{\beta_{i+1} \cdots \beta_j}{\alpha_i \cdots \alpha_j} = \frac{1}{\alpha_i} \frac{\prod_{n=i+1}^j n}{\prod_{n=i+1}^j (n+2)} = \frac{2(i+1)^2}{(j+1)(j+2)}$$

for all $j \geq i$. This provides the desired formula for the entries of $(R_{0,1}^+)^{-1}$. Finally, using Definition 5.2 with $\omega_{m,n} = (1 + 2n + |m|)^s$, we have

$$\|(R_{0,1}^+)^{-1}\|_{B(V_s^{0,2}, V_{s-1}^{0,1})} = \max_{j \in \mathbb{N}_0} \left\{ \frac{1}{(2j+3)^s} \sum_{i=0}^j \frac{2(i+1)^2}{(j+1)(j+2)} (2i+2)^{s-1} \right\} \quad (43)$$

As the sum is monotonic, we may bound it above by an integral, from which we may see that $\|(R_{0,1}^+)^{-1}\|_{B(V_s^{0,2}, V_{s-1}^{0,1})} < \infty$ for all $s \geq 0$. For calculating the norm with $s = 0$ this reduces to:

$$\|(R_{0,1}^+)^{-1}\|_{B(V_0^{0,2}, V_{-1}^{0,1})} = \max_{j \in \mathbb{N}_0} \left\{ \sum_{i=0}^j \frac{(i+1)}{(j+1)(j+2)} \right\} = \frac{1}{2}.$$

In order to compute the inverse of $R_{0,0}^+$, we use the above reasoning with $\alpha_i = \frac{i+1}{2i+1}$ and $\beta_i = \frac{i}{2i+1}$ and obtain the entries of the inverse using (42). \square

Acknowledgement This work was conducted during the thematic semester titled ‘‘Computational Dynamics - Analysis, Topology & Data’’, supported by the Centre de Recherches Mathématiques at the University of Montreal and the Simons Foundation. The authors sincerely thank these institutions for their funding and for providing the opportunity to explore this research. AT is also partially supported by the Top Runners in Strategy of Transborder Advanced Researches (TRiSTAR) program conducted as the Strategic Professional Development Program for Young Researchers by the MEXT, and by JSPS KAKENHI Grant Numbers JP22K03411, JP21H01001, and JP24K00538.

Declaration of generative AI and AI-assisted technologies in the writing process During the preparation of this work, the authors used ChatGPT to assist in refining the English wording and enhancing the clarity of the presented content. After using this tool/service, the authors reviewed and edited the content as needed and take full responsibility for the content of the publication.

References

- [AGK21] Gianni Arioli, Filippo Gazzola, and Hans Koch. Uniqueness and bifurcation branches for planar steady Navier-Stokes equations under Navier boundary conditions. *J. Math. Fluid Mech.*, 23(3):Paper No. 49, 20, 2021.
- [AK10] Gianni Arioli and Hans Koch. Integration of dissipative partial differential equations: a case study. *SIAM J. Appl. Dyn. Syst.*, 9(3):1119–1133, 2010.
- [AK19] Gianni Arioli and Hans Koch. Non-radial solutions for some semilinear elliptic equations on the disk. *Nonlinear Analysis*, 179:294–308, 2019.
- [AK24] Gianni Arioli and Hans Koch. Periodic and quasiperiodic waves on the sphere. *SIAM Journal on Applied Dynamical Systems*, 23(4):2769–2792, 2024.
- [Bar02] Roberto Barrio. Rounding error bounds for the Clenshaw and Forsythe algorithms for the evaluation of orthogonal polynomial series. *Journal of computational and applied mathematics*, 138(2):185–204, 2002.

- [BC24] Maxime Breden and Hugo Chu. Constructive proofs for some semilinear PDEs on $H^2(e^{|x|/4}, \mathbb{R}^d)$. Preprint, 2024.
- [BCLGS22] Tristan Buckmaster, Gonzalo Cao-Labora, and Javier Gómez-Serrano. Smooth imploding solutions for 3D compressible fluids. *arXiv preprint arXiv:2208.09445*, 2022.
- [BEKS17] Jeff Bezanson, Alan Edelman, Stefan Karpinski, and Viral B Shah. Julia: A fresh approach to numerical computing. *SIAM Review*, 59(1):65–98, 2017.
- [BLC84] Lawrence C Biedenharn, James D Louck, and Peter A Carruthers. *Angular momentum in quantum physics: theory and application*. 1984.
- [Bog14] Ignace Bogaert. Iteration-free computation of gauss–legendre quadrature nodes and weights. *SIAM Journal on Scientific Computing*, 36(3):A1008–A1026, 2014.
- [Boy01] John P Boyd. *Chebyshev and Fourier spectral methods*. Courier Corporation, 2001.
- [BVO⁺20] Keaton J Burns, Geoffrey M Vasil, Jeffrey S Oishi, Daniel Lecoanet, and Benjamin P Brown. Dedalus: A flexible framework for numerical simulations with spectral methods. *Physical Review Research*, 2(2):023068, 2020.
- [BW99] Max Born and Emil Wolf. *Principles of Optics: Electromagnetic Theory of Propagation, Interference and Diffraction of Light*. Cambridge University Press, Cambridge, UK, 7th edition, 1999.
- [BY11] John P Boyd and Fu Yu. Comparing seven spectral methods for interpolation and for solving the Poisson equation in a disk: Zernike polynomials, Logan–Shepp ridge polynomials, Chebyshev–Fourier series, cylindrical Robert functions, Bessel–Fourier expansions, square-to-disk conformal mapping and radial basis functions. *Journal of Computational Physics*, 230(4):1408–1438, 2011.
- [Cad24] Matthieu Cadiot. ZernikePolynomials.jl. 2024. <https://github.com/matthieucadiot/ZernikePolynomials.jl>.
- [CH22] Jiajie Chen and Thomas Y Hou. Stable nearly self-similar blowup of the 2D Boussinesq and 3D Euler equations with smooth data. *arXiv preprint arXiv:2210.07191v2*, 2022.
- [CW18] Jacek Cyranka and Thomas Wanner. Computer-assisted proof of heteroclinic connections in the one-dimensional Ohta-Kawasaki Model. *SIAM J. Appl. Dyn. Syst.*, 17(1):694–731, 2018.
- [DS19] Stephanie Dodson and Bjorn Sandstede. Determining the source of period-doubling instabilities in spiral waves. *SIAM Journal on Applied Dynamical Systems*, 18(4):2202–2226, 2019.
- [FGLdlL17] Jordi-Lluís Figueras, Marcio Gameiro, Jean-Philippe Lessard, and Rafael de la Llave. A framework for the numerical computation and a posteriori verification of invariant objects of evolution equations. *SIAM J. Appl. Dyn. Syst.*, 16(2):1070–1088, 2017.
- [For57] George E. Forsythe. Generation and use of orthogonal polynomials for data-fitting with a digital computer. *J. Soc. Indust. Appl. Math.*, 5:74–88, 1957.

- [GL10] Marcio Gameiro and Jean-Philippe Lessard. Analytic estimates and rigorous continuation for equilibria of higher-dimensional PDEs. *J. Differential Equations*, 249(9):2237–2268, 2010.
- [GR00] I. S. Gradshteyn and I. M. Ryzhik. *Table of integrals, series, and products*. Academic Press, Inc., San Diego, CA, sixth edition, 2000. Translated from the Russian, Translation edited and with a preface by Alan Jeffrey and Daniel Zwillinger.
- [GS19] Javier Gómez-Serrano. Computer-assisted proofs in PDE: a survey. *SeMA J.*, 76(3):459–484, 2019.
- [GW69] Gene H. Golub and John H. Welsch. Calculation of gauss quadrature rules. *Mathematics of Computation*, 23(106):221–230, 1969.
- [HH23] Thomas Y Hou and De Huang. Potential singularity formation of incompressible axisymmetric euler equations with degenerate viscosity coefficients. *Multiscale Modeling & Simulation*, 21(1):218–268, 2023.
- [HL08] Thomas Y Hou and Congming Li. Dynamic stability of the three-dimensional axisymmetric Navier-Stokes equations with swirl. *Communications on Pure and Applied Mathematics: A Journal Issued by the Courant Institute of Mathematical Sciences*, 61(5):661–697, 2008.
- [Hou23] Thomas Y. Hou. Potentially singular behavior of the 3d Navier–Stokes equations. *Foundations of Computational Mathematics*, 23(6):2251–2299, 2023.
- [HT13] Nicholas Hale and Alex Townsend. Fast and accurate computation of Gauss–Legendre and Gauss–Jacobi quadrature nodes and weights. *SIAM Journal on Scientific Computing*, 35(2):A652–A674, 2013.
- [Jan14] AJEM Janssen. Zernike expansion of derivatives and Laplacians of the Zernike circle polynomials. *JOSA A*, 31(7):1604–1613, 2014.
- [Jaq19] Jonathan Jaquette. A proof of Jones’ conjecture. *J. Differential Equations*, 266(6):3818–3859, 2019.
- [Kan85] Yūichi Kanjin. Banach algebra related to disk polynomials. *Tohoku Mathematical Journal*, 37(3):395 – 404, 1985.
- [Kar93] Alain Karma. Spiral breakup in model equations of action potential propagation in cardiac tissue. *Physical review letters*, 71(7):1103, 1993.
- [Kar94] Alain Karma. Electrical alternans and spiral wave breakup in cardiac tissue. *Chaos: An Interdisciplinary Journal of Nonlinear Science*, 4(3):461–472, 1994.
- [KNWN09] Myoungnyoung Kim, Mitsuhiro T. Nakao, Yoshitaka Watanabe, and Takaaki Nishida. A numerical verification method of bifurcating solutions for 3-dimensional Rayleigh-Bénard problems. *Numer. Math.*, 111(3):389–406, 2009.
- [Koo78] Tom Koornwinder. Positivity proofs for linearization and connection coefficients of orthogonal polynomials satisfying an addition formula. *Journal of the London Mathematical Society*, 2(1):101–114, 1978.

- [KSW96] Hans Koch, Alain Schenkel, and Peter Wittwer. Computer-assisted proofs in analysis and programming in logic: a case study. *SIAM Rev.*, 38(4):565–604, 1996.
- [Lan82] Oscar E. Lanford, III. A computer-assisted proof of the Feigenbaum conjectures. *Bull. Amer. Math. Soc. (N.S.)*, 6(3):427–434, 1982.
- [LNO22] Xuefeng Liu, Mitsuhiro T. Nakao, and Shin’ichi Oishi. Computer-assisted proof for the stationary solution existence of the Navier-Stokes equation over 3D domains. *Commun. Nonlinear Sci. Numer. Simul.*, 108:Paper No. 106223, 15, 2022.
- [LO13] Xuefeng Liu and Shin’ichi Oishi. Verified eigenvalue evaluation for the Laplacian over polygonal domains of arbitrary shape. *SIAM J. Numer. Anal.*, 51(3):1634–1654, 2013.
- [Lop94] JM Lopez. On the bifurcation structure of axisymmetric vortex breakdown in a constricted pipe. *Physics of Fluids*, 6(11):3683–3693, 1994.
- [LS98] JM Lopez and Jie Shen. An efficient spectral-projection method for the Navier–Stokes equations in cylindrical geometries: I. axisymmetric cases. *Journal of Computational Physics*, 139(2):308–326, 1998.
- [MB02] Andrew J Majda and Andrea L Bertozzi. *Vorticity and incompressible flow*. Cambridge University Press, Cambridge, 2002.
- [MM95a] T Matsushima and PS Marcus. A spectral method for polar coordinates. *Journal of Computational Physics*, 120(2):365–374, 1995.
- [MM95b] Konstantin Mischaikow and Marian Mrozek. Chaos in the Lorenz equations: a computer-assisted proof. *Bull. Amer. Math. Soc. (N.S.)*, 32(1):66–72, 1995.
- [Moo66] Ramon E. Moore. *Interval analysis*. Prentice-Hall Inc., Englewood Cliffs, N.J., 1966.
- [Nak01] Mitsuhiro T. Nakao. Numerical verification methods for solutions of ordinary and partial differential equations. volume 22, pages 321–356. 2001. International Workshops on Numerical Methods and Verification of Solutions, and on Numerical Function Analysis (Ehime/Shimane, 1999).
- [NHW05] M. T. Nakao, K. Hashimoto, and Y. Watanabe. A numerical method to verify the invertibility of linear elliptic operators with applications to nonlinear problems. *Computing*, 75(1):1–14, 2005.
- [Nol76] R. J. Noll. Zernike polynomials and atmospheric turbulence. *Journal of the Optical Society of America*, 66(3):207–211, 1976.
- [NPW19] Mitsuhiro T. Nakao, Michael Plum, and Yoshitaka Watanabe. *Numerical verification methods and computer-assisted proofs for partial differential equations*, volume 53 of *Springer Series in Computational Mathematics*. Springer, Singapore, [2019] ©2019.
- [OLBC10] Frank Olver, Daniel Lozier, Ronald Boisvert, and Charles Clark. *The NIST Handbook of Mathematical Functions*. Cambridge University Press, New York, NY, 2010-05-12 00:05:00 2010.
- [Rum10] Siegfried M. Rump. Verification methods: rigorous results using floating-point arithmetic. *Acta Numer.*, 19:287–449, 2010.

- [SB14] David P. Sanders and Luis Benet. `Intervalarithmetic.jl`, 2014.
- [She00] Jie Shen. A new fast Chebyshev–Fourier algorithm for Poisson-type equations in polar geometries. *Applied Numerical Mathematics*, 33(1-4):183–190, 2000.
- [SSW99] B Sandstede, A Scheel, and C Wulff. Bifurcations and dynamics of spiral waves. *Journal of nonlinear science*, 9:439–478, 1999.
- [Sto93] Ulrike Storck. Verified calculation of the nodes and weights for gaussian quadrature formulas. *Interval Computations*, 4:114–124, 1993.
- [STW11] Jie Shen, Tao Tang, and Li-Lian Wang. *Spectral methods: algorithms, analysis and applications*, volume 41. Springer Science & Business Media, 2011.
- [TLO13] Akitoshi Takayasu, Xuefeng Liu, and Shin’ichi Oishi. Verified computations to semi-linear elliptic boundary value problems on arbitrary polygonal domains. *Nonlinear Theory and Its Applications, IEICE*, 4(1):34–61, 2013.
- [Tuc99] Warwick Tucker. The Lorenz attractor exists. *C. R. Acad. Sci. Paris Sér. I Math.*, 328(12):1197–1202, 1999.
- [Tuc21] Warwick Tucker. A rigorous ODE Solver and Smale’s 14th Problem. *Foundations of Computational Mathematics*, 2(1):53–117–117, 2002-12-21.
- [Tuc11] Warwick Tucker. *Validated numerics*. Princeton University Press, Princeton, NJ, 2011. A short introduction to rigorous computations.
- [VBL⁺16] Geoffrey M Vasil, Keaton J Burns, Daniel Lecoanet, Sheehan Olver, Benjamin P Brown, and Jeffrey S Oishi. Tensor calculus in polar coordinates using jacobi polynomials. *Journal of Computational Physics*, 325:53–73, 2016.
- [vdBBC⁺18] Jan Bouwe van den Berg, István Balázs, Julien Courtois, János Dudás, Anett Vörös-Kiss, Xi Yuan Yin, JF Williams, and Jean-Philippe Lessard. Computer-assisted proofs for radially symmetric solutions of pdes. *Journal of Computational Dynamics*, 5(1&2):61–80, 2018.
- [vdBBLvV21] Jan Bouwe van den Berg, Maxime Breden, Jean-Philippe Lessard, and Lennaert van Veen. Spontaneous periodic orbits in the Navier-Stokes flow. *J. Nonlinear Sci.*, 31(2):Paper No. 41, 64, 2021.
- [vdBDL22] Jan Bouwe van den Berg, Gabriel William Duchesne, and Jean-Philippe Lessard. Rotation invariant patterns for a nonlinear Laplace-Beltrami equation: A Taylor-Chebyshev series approach. *Journal of Computational Dynamics*, 9(2):253–278, 2022.
- [vdBJ18] Jan Bouwe van den Berg and Jonathan Jaquette. A proof of Wright’s conjecture. *J. Differential Equations*, 264(12):7412–7462, 2018.
- [vdBL15] Jan Bouwe van den Berg and Jean-Philippe Lessard. Rigorous numerics in dynamics. *Notices Amer. Math. Soc.*, 62(9):1057–1061, 2015.
- [vdBW19] Jan Bouwe van den Berg and J. F. Williams. Rigorously computing symmetric stationary states of the Ohta-Kawasaki problem in three dimensions. *SIAM J. Math. Anal.*, 51(1):131–158, 2019.

- [Wal65] J. L. Walsh. *Interpolation and approximation by rational functions in the complex domain*, volume Vol. XX of *American Mathematical Society Colloquium Publications*. American Mathematical Society, Providence, RI, fourth edition, 1965.
- [WPN09] Yoshitaka Watanabe, Michael Plum, and Mitsuhiro T. Nakao. A computer-assisted instability proof for the Orr-Sommerfeld problem with Poiseuille flow. *ZAMM Z. Angew. Math. Mech.*, 89(1):5–18, 2009.
- [Wun22] Jonathan Matthias Wunderlich. *Computer-assisted Existence Proofs for Navier-Stokes Equations on an Unbounded Strip with Obstacle*. PhD thesis, Karlsruher Institut für Technologie (KIT), 2022.
- [WZ20] Daniel Wilczak and Piotr Zgliczyński. A geometric method for infinite-dimensional chaos: symbolic dynamics for the Kuramoto-Sivashinsky PDE on the line. *J. Differential Equations*, 269(10):8509–8548, 2020.
- [YN93] Nobito Yamamoto and Mitsuhiro T. Nakao. Numerical verifications of solutions for elliptic equations in nonconvex polygonal domains. *Numer. Math.*, 65(4):503–521, 1993.
- [Zer34] von F. Zernike. Beugungstheorie des schneidenverfahrens und seiner verbesserten form, der phasenkontrastmethode. *Physica*, 1(7):689–704, May 1934.
- [ZM01] Piotr Zgliczyński and Konstantin Mischaikow. Rigorous numerics for partial differential equations: the Kuramoto-Sivashinsky equation. *Found. Comput. Math.*, 1(3):255–288, 2001.